Hydraulics Research
Wallingford

A MATHEMATICAL MODEL OF MUD TRANSPORT IN DEEP PARTIALLY MIXED CANALIZED ESTUARIES

James Rodger
Nicholas Odd

Report No SR 37
March 1985

Registered Office: Hydraulics Research Limited,
Wallingford, Oxfordshire OX10 8BA.
Telephone: 0491 35381. Telex: 848552

ABSTRACT

The report describes the theory and first application of a new type of multi-layer model which can simulate the interaction of tidal and fluvial flows on saline intrusion, mud transport and siltation in deep partially mixed canalised estuaries. The physics of the various interacting processes are described. Novel aspects include the method of calculating vertical mixing and the modelling of the formation of a thin layered slack water deposit.

The derivation of the basic differential equations and the numerical solution technique are described in the report.

The capability of the model is described with examples from an application to the Brisbane river estuary. It was used to predict siltation caused by individual river floods. The results were analyses using statistical methods to predict long term siltation rates over a period of 50 years.

The model, which represents the state of the art for its type, is important because it allows planners to predict the effect of engineering works on mud transport and siltation in a common type of estuary.

The model is at present being used to predict the effect of proposed modifications to the residual flows over Teddington weir on the pattern of mud transport and siltation in the Thames Estuary, for the Thames Water Authority and the Port of London Authority.

The calibration procedure could be simplified and the predictive ability of the model could be improved by undertaking further research into better methods of modelling the density profile of the unconsolidated slack water deposits.

There is a need to develop a three-dimensional mud transport model to predict conditions in berthing areas and tidal basins.

This report describes work funded by the Department of the Environment under Research Contract DGR/465/35, funded by the Department of Transport from April 1982 to March 1984 and thereafter by the Department of the Environment. Any opinions expressed in this report are not necessarily those of the funding Departments. The DOE (ESPU) nominated officer was Mr A J M Harrison. The work was carried out by Dr J G Rodger and Mr N V M Odd of the Tidal Computations Group in the Tidal Engineering Department of Hydraulics Research, Wallingford, under the management of Mr M F C Thorn. It is published with the permission of the Department of the Environment.

CONTENTS

Page

1 INTRODUCTION

2 MATHEMATICAL MODELS

3 TIDAL FLOW PROCESSES

4 THE MODEL

4.1 Basic differential equations

5 VERTICAL EXCHANGE

5.1 Effect of Richardson number on solute mixing length

6 BOUNDARY CONDITIONS

7 NUMERICAL SOLUTION TECHNIQUE

7.1 Layer averaged equations of motion
7.2 Finite difference representation

8 PHYSIO-CHEMICAL PROPERTIES OF MUD

9 SETTLING VELOCITY OF MUD FLOCS

10 FORMATION OF A MUD DEPOSIT

11 EROSION AND SUSPENSION OF MUD

11.1 Sand-mud mixtures
11.2 Sand in suspension

12 APPLICATION TO THE BRISBANE RIVER ESTUARY

13 SUSPENDED MUD LOAD OF THE RIVER

14 SIMULATION OF CONDITIONS DURING THE DRY SEASON

15 SIMULATION OF CONDITIONS DURING AND IMMEDIATELY AFTER A FLUVIAL FLOOD

16 TRAPPING EFFICIENCY OF THE ESTUARY

17 ANALYSIS OF FLOOD DATA 1927-1972

17.1 Results
17.2 Flood 1
17.3 Flood 2
17.4 Floods 3 and 4

18 TRENDS IN THE MODEL PREDICTIONS

19 LONG TERM AVERAGE ANNUAL RATE OF SILTATION

20 CONCLUSIONS

21 ACKNOWLEDGEMENTS

22 REFERENCES

TABLES

1. Statistics of flood events simulated in the model
2. Mass balance of mud transport in the estuary
3. Hindcast mud siltation 1927-1972

FIGURES

1. Interaction of tidal processes
2. Gravitational circulation in the Mersey estuary
3. Distribution of suspended mud in the Thames estuary
4. Typical velocity, salinity, R_i and mixing length profiles
5. Two-dimensional finite difference grid
6. Schematic representation of slack water mud deposits
7. Schematic representation of sub-surface mixed sand and mud deposits
8. Brisbane river location plan
9. Port of Brisbane location plan
10. Synthesised neap spring tidal cycle at West Inner Bar
11. Schematic representation of the Brisbane river estuary
12. Undisturbed vibro bed cores
13. Comparison of simulated and observed tidal amplitudes
14. Comparison of simulated and observed velocity profiles in the port area - dry season
15. Comparison of simulated and observed velocities at bed surface in port area - dry season
16. Comparison of simulated and observed mud concentrations in the port area - dry season
17. Tide-averaged suspended solids and salinities - model and observations in dry season
18. Hindcast mud siltation pattern - 1977 dry season
19. First fluvial flood hydrograph - 1978 wet season
20. 1600 hours 4th April 1978
21. 1300 hours 7th April 1978
22. Comparison of simulated and observed salinities in Hamilton Reach 1-12/4/78
23. Comparison of simulated and observed velocity profiles in Hamilton Reach 11/4/78
24. Pattern of deposition and erosion in Hamilton Reach 2-12/4/78
25. Schematic representation of sedimentation processes in the Brisbane river estuary - wet season
26. Flood hydrographs
27. Flood frequency as a function of flood volume
28. Predicted longitudinal distribution of mud siltation - Flood 1
29. Predicted longitudinal distribution of mud siltation - Flood 2
30. Predicted longitudinal distribution of mud siltation - Flood 3
31. Predicted longitudinal distribution of mud siltation - Flood 4
32. Trapping efficiency of the estuary a function of fluvial flood volume
33. Net movement of mud into the estuary a function of fluvial flood volume

1 INTRODUCTION

Many of the world's major cities and largest ports are sited on artificially deepened and canalized estuaries. The capital dredging works required to enlarge navigation channels are major engineering projects. The periodic removal of siltation in such artificial channels is a serious drain on the budget of many ports. There is therefore a need for engineers who are planning to deepen the approach channel to a port to be able to predict the future siltation rates and hence the cost of maintenance dredging.

The lower reaches of an estuary are gradually trained and deepened to accommodate the increasing size of vessels using a port. Maintenance dredging is then often reduced in the landward reaches of an estuary as the deep draft vessels cease to use the upstream berths. The construction of reservoirs, diversions and extractions for water supply and irrigation purposes may reduce the fluvial inflows to such an extent as to change the pattern of siltation in an estuary.

Besides governing the distribution of siltation, the pattern of mud transport also determines the transport and accumulation of particulate pollutants and the penetration of light and hence the health of the eco-system in an estuary.

The accumulative and interactive effect of engineering works built in a piece meal fashion over a long period of time make it increasingly more difficult to implement good overall planning and design of works in an estuary.

The mathematical model described in this report is capable of providing planners with useful predictions for a range of engineering problems associated with deep canalized estuaries.

A canalized estuary is defined as a body of water, narrow with respect to its length, which moves under the influence of external tidal forces and fluvial flows. The outfall of a river is the meeting place of fresh water and sea water, which gives rise to a variety of important phenomena, such as stratification and gravitational circulation and these effects are enhanced in a deep estuary. The depth of an estuary is measured in absolute terms and relative to the tidal range where for practical purposes, one can assume that a deep estuary is one in which the mean depths are in excess of about 10m and the tidal range to mean depth ratio is less than about 0.4. The tide usually propagates through the deep regions of such

estuaries without significant distortion due to shallow water effects.

The silting material may consist of bulky cohesive mud, clean granular sand or a mixture of both. The sediments may be brought down during fluvial floods or reworked marine sediments brought up from the sea by the tide. There is a wide variation in the geography of individual tidal channel systems and in the combination of different tidal and fluvial regimes. The problem of determining which of the main factors which influence siltation in a navigation channel has in the past been the cause of heated debate by engineers and even politicians. In some cases works have been carried out which have had the opposite effect to that which was intended due to ignorance of the processes involved by the designer of the works. However, basic physical principles can be applied to analyse the process of siltation in each particular situation, and the advent of the computer has enabled engineers to formulate mathematical models based on these principles. These models can be used to simulate and predict the movement of water, salt and sediment in tidal channels and hence the pattern of siltation.

2 MATHEMATICAL MODELS

A mathematical model in the context of siltation in estuaries is the systematic calculation of the movement of water, salt and sediments element by element throughout the estuary at successive time intervals. The main features of tidal motion are determinate and respond to basically simple laws of physics. That is to say, the imposition of an external force on a body of water must result in its acceleration, and the net amount of water that leaves or enters an element equals the amount stored or lost by it. Similarly, laws governing the conservation of matter may be applied to the motion of dissolved salt and suspended sediment, but certain aspects of their motion can, as yet, only be defined by empirical relationships. Models based on the laws of physics are termed deterministic models, whereas models based wholely on empirical relationships are termed functional models. Most sediment transport models are hybrid since they contain empirical relationships which have an important influence on the solution and the predictive ability of these hybrid models is limited by the range of conditions for which their empirical functions are known to hold true. The interaction of the main processes causing siltation in a tidal channel are shown schematically in Figure 1.

The first complete mathematical model of mud transport and siltation in an estuary was developed by Odd and

Owen on the Thames estuary in 1968 (Ref 1). Since then, HR have developed and successfully used a series of increasingly complex numerical models (Ref 2) to simulate mud and sand transport in different types of estuaries. However, this report is only concerned with simulating conditions in narrow estuarine channels.

3 TIDAL FLOW PROCESSES

The main forcing motions causing sediment transport in estuaries are the external tide and fluvial inflows. An essential prerequisite of any sediment transport calculation is the ability to simulate and predict the pattern of primary tidal currents and equally importantly the secondary depth dependant and partly non-tidal currents. The strength of the primary tidal currents depends on the tidal range to depth ratio, the resonance characteristics of the estuary and its rate of narrowing.

One of the most important aspects of the hydraulics of deep estuaries is the longitudinal gravitational circulation that is driven by the longitudinal density gradients within the estuary. The magnitude of the longitudinal pressure gradient, which causes the gravitational circulation, is a function of the slope of the mean tide level and the vertical variation in the tide average longitudinal density gradient as follows:

$$\left(\frac{dp}{dx}\right)_z = g\,\bar{\rho}_s\frac{d\eta_o}{dx} + g\int_z^{\eta}\frac{\partial\bar{\rho}}{\partial x}\,.\,dz \qquad (3.1)$$

where ρ_s is the density of the surface water (kg/m^3)
g is the acceleration of gravity($9.81 m^3 s^{-2}$).

The strength of the gravitational circulation varies directly with the magnitude of the product of the depth and the longitudinal density gradient. It is reduced by vertical mixing, which is usually heavily damped in stratified flows, and by energy dissipation of the bed, which is increased by the occurrence of high tidal velocities in the lower layers. The net landward pressure gradient and the net landward residual flow at the bed disappear at a null point in the estuary where the two terms on the right hand side of equation 3.1 cancel each other out. The pattern of gravitational circulation will vary according to the degree of stratification, but it is not dependent on the existence of vertical density stratification. Many deep estuaries with weak or negligible vertical stratification have strong gravitational circulations. The longitudinal density gradients tend to distort the

shape of the velocity profile on the flood and ebb phases of the tide and thereby induce a net landward longitudinal movement of water in the bed layers seaward of the null point. There is a corresponding net seaward flow of water in the surface layers of the estuary giving rise to a two-layer circulation. The level at which the residual currents reverse direction varies with position in the estuary. If the tidal range is significant compared to the mean depth, there may be a three-layer structure with a small net landward movement of water in the layers above mean tide level.

Generally it is important to be able to calculate the vertical structure of the flow and suspended and dissolved concentration distributions. This requires the use of a layered or x-z-t model. If the rate of tidal mixing is small compared to the influx of fluvial water, a surface layer of brackish water will form with a fairly distinct interface from the more saline water below. If the interface is very sharp it may be necessary to employ a two-layer model rather than a multi-layer model because of the inability of the latter model to resolve the gradients at the interface.

The gravitational circulation in a deep estuary tends to contain the suspended sediments in a relatively well defined turbid zone close to the null point. If the peak bed stresses are low enough, mud shoals will form in this region which is often called the mud reaches of an estuary.

4 THE MODEL

The model, although referred to as a multi-layer model, can perform two different types of calculation depending on the type or part of the estuary being modelled:

(a) In reaches where the vertical structure of the estuary is important the model solves the two-dimensional (width-averaged) equations of motion describing conservation of volume, momentum, salt and suspended solids.

(b) In well mixed reaches the model solves the one-dimensional or bulk flow conservation equations.

The type of calculation to be performed in any part of an estuary is fixed before the model is applied and, in looped or branched channel networks, the model may comprise several reaches of types (a) and (b). The model is constructed in this way to minimise computational time and computer storage requirements when modelling long or complex estuaries containing

reaches with homogeneous flow far from a region of interest.

4.1 Basic differential equations

The equations used to describe unsteady laterally averaged flow are:

Conservation of momentum:

$$\frac{\delta uB}{\delta t} + \frac{\delta u^2 B}{\delta x} + \frac{\delta uwB}{\delta z} + \frac{B}{\rho}\frac{\delta P}{\delta x} = \frac{1}{\rho}\frac{\delta \tau B}{\delta z} \qquad (4.1)$$

where B is the width of the channel (m)
n is the horizontal velocity (m/s)
w is the vertical velocity (m/s)
T is the Reynolds stress (N/m^2)

Hydrostatic pressure approximation:

$$\frac{\delta P}{\delta z} + \rho g = 0 \qquad (4.2)$$

Conservation of volume:

$$\frac{\delta uB}{\delta x} + \frac{\delta wB}{\delta z} = 0 \qquad (4.3)$$

Conservation of mud:

$$\frac{\delta cB}{\delta t} + \frac{\delta ucB}{\delta x} + \frac{\delta (w-\omega)cB}{\delta z} - \frac{\delta}{\delta x}\left(BD\frac{\delta c}{\delta x}\right) = \frac{\delta BF}{\delta z} + \frac{dm}{dt} \qquad (4.4)$$

where c is the concentration of suspended mud
w is the settling velocity of mud (m/s)
F is the vertical turbulent flux of mud ($kg/m^2/s$)

Conservation of salt:

$$\frac{\delta sB}{\delta t} + \frac{\delta usB}{\delta x} + \frac{\delta wsB}{\delta z} - \frac{\delta}{\delta x}\left(BD\frac{\delta s}{\delta x}\right) = \frac{\delta BF_s}{\delta z} \qquad (4.5)$$

where s is the salinity (kg/m^3)

$$\rho = 1000 + 0.76s + 0.62C \qquad (4.6)$$

$\frac{dm}{dt}$ represents deposition or erosion in the bed layer.

Longitudinal derivatives and correlations of turbulent fluctuations have been neglected. However, it was

thought necessary to include the longitudinal dispersion terms in equations (4.4) and (4.5) to allow for the enhanced longitudinal mixing resulting from lateral variations in concentration and the mean longitudinal velocity component. The Boussinesq approximation has been made so variations in density in the momentum equation have been neglected except in the pressure term.

5 VERTICAL EXCHANGE

The vertical exchange of momentum through the agency of turbulent mixing gives rise to internal stresses in the flow which affect the shape of the velocity profile and hence the transport of sediment along the estuary. The strength of the tidal currents and the degree of stratification also determine the rate at which suspended sediment is lifted from the lower to the upper layers of the flow by vertical turbulent exchange. Suspended mud flocs settle downwards towards the bed at a rate which is dependent on their size and submerged density.

Over the past decade, HR have put a major research effort in developing practical theories for describing vertical turbulent exchange in stratified tidal flows. The universal coefficients in the semi-empirical functions were derived from the analysis of field observations in real estuaries. The theories employed by HR are based on the concept of mixing lengths which are considered to be adequate for describing vertical turbulent exchange in gradually varying tidal flows (Ref 3). In the authors' opinion it is not yet practical to incorporate theoretically more sophisticated turbulence models due to the large number of non-constant coefficients which are necessary to deal with stratified flows.

The turbulent horizontal velocity (u), vertical velocity (w), and salinity (s) can be expressed as a sum of a turbulent mean component (denoted by -) and a fluctuating component (denoted by ') by defining:

$$u = \bar{u} + u'$$
$$w = \bar{w} + w' \qquad (5.1)$$
$$s = \bar{s} + s'$$

where, for example $\bar{u} = \frac{1}{T}\int_{t}^{t+T} u\,dt$ where T is long compared to the period of the turbulent fluctuations and, by definition $\bar{u}' = \bar{w}' = \bar{s}' = 0$.

(For the two-dimensional analysis, the lateral velocity component is neglected).

The horizontal Reynolds stress is defined as:

$$\tau_{xz} = - \bar{\rho}\, \bar{u}'\bar{w}' \qquad (5.2)$$

and the vertical mass flux is

$$F_z = \bar{w}'\bar{s}' \qquad (5.3)$$

where $\bar{\rho}$ is the mean density. Following Prandtl, the Reynolds stress can be written as:

$$\tau_{xz} = \bar{\rho} \ell_m^2 \frac{\partial \bar{u}}{\partial z} \frac{\partial \bar{u}}{\partial z} \qquad (5.4)$$

and the mass flux can be written as:

$$F_z = \ell_m \ell_c \frac{\partial \bar{u}}{\partial z} \frac{\partial \bar{s}}{\partial z} \qquad (5.5)$$

where ℓ_m is the Prandtl mixing length for momentum and ℓ_c is the mixing length for dissolved and suspended matter.

In homogeneous conditions, if a logarithmic velocity profile and a linearly varying shear stress are assumed, the mixing length for momentum at any height (z) above the bed can be expressed in terms of the total depth of flow as:

$$\ell_m = Kz \left(1 - \frac{z}{d}\right)^{\frac{1}{2}} \qquad (5.6)$$

where K is von Karmen's constant.

In the line with many researchers, Odd and Roger (Ref 4) proposed that in stratified conditions, the mixing length would be modified by buoyancy effects and could be written in terms of the homogeneous mixing length (l_{mo}) and a function of the gradient Richardson number (R_i) as:

$$l_m = l_{mo}\, f\,(R_i) \qquad (5.7)$$

where $R_i = \frac{-g}{\bar{\rho}} \left(\frac{\partial \bar{\rho}}{\partial z}\right) / \left(\frac{\partial \bar{u}}{\partial z}\right)^2$. (5.8)

They determined the function $f(R_i)$ indirectly from a large set of data obtained under highly stratified conditions in the Great Ouse and found the function to take on two forms depending on whether the Richardson number increased monotonically from bed to surface or had a maximum value in the body of the flow. The identification of two forms for the damping function was considered significant because, two forms of the damping function differentiate between flows with perhaps the same global Richardson number but with entirely different internal structures. This earlier work identified that for the stratified estuarine flows under consideration, the presence of a peak Richardson number - typically at the position of a peak in the density gradient - had a limiting effect on the mixing throughout the entire flow depth.

5.1 Effect of Richardson number on solute mixing length

In 1957, Ellison presented a theory that predicted the dependence of the turbulent Schmidt Number (l_c/l_m) on the gradient Richardson Number and a critical flux Richardson Number, Rf_c, which when simplified and expressed in terms of mixing length is:

$$\frac{l_c}{l_m} = \frac{1 - \frac{l_c}{l_m}\frac{Ri}{Rf_c}}{1 - \frac{l_c}{l_m} Ri} 2 \qquad (5.9)$$

Ellison's function imposes the following conditions on the value of the flux Richardson Number, $Rf = R_{i\frac{l_c}{l_m}}$ and the turbulent Schmidt Number l_c/l_m.

Namely, that as Ri increases, Rf increases towards a maximum value, Rf_c, and that l_c/l_m decreases from unity and tends to zero. Ellison argued that Rf_c had a value of about 0.15. In other words, only a small fraction of the turbulent energy generated by internal shearing is available for increasing the potential energy of the flow. Ellison's explanation of the relative inefficiency of mass transfer in stratified conditions is that a displaced fluid particle tends to return to its equilibrium level before it has had time to mix with its surroundings. A parcel of water can transfer its momentum during a brief excursion without mixing with its surroundings through pressure

fluctuations but in order to transfer matter it must mix with its surrounding water.

A set of mixing length functions for calculating the vertical turbulent exchange of momentum and solutes in gradually varying turbulent stratified flows is proposed in which the momentum mixing length is:

1. In quasi-equilibrium with the instantaneous velocity and density profiles

2. Insensitive to large variations in the longitudinal density gradients

3. Generally uniform throughout the depth except near the bed and the surface where the homogeneous profile prevails.

4. A strong function of the magnitude and relative depth of the peak gradient Richardson Number

5. A function of the local Ri value in the absence of a peak in the Ri profile.

6. Sensitive to the contribution of suspended solids to the total bulk density of the flow for low Ri values

7. Effectively independent of variations in the value of Ri when it exceeds unity.

The solute mixing length, l_c, is generally a fraction of the local momentum mixing length and indirectly a function of both the peak Ri value (if present) and the local Ri value. The instantaneous mixing length profile in the model is calculated in the following manner:

1. Evaluate the vertical bulk density distribution including dissolved and suspended matter

2. Evaluate the gradient Richardson Number, Ri, smooth the Ri profile if necessary. The amount of smoothing is a matter of judgement

3. Examine the Ri profile from the bed upwards for the existence of a well defined peak

4. If the Ri value increases continuously from the bed upwards to a level bounding 75% of the depth of the flow or greater, the momentum mixing length, l_m, is:

$$l_m(z) = 0.4z \left(1 - \frac{z}{d}\right)^{\frac{1}{2}} \left[1 + \beta \, Ri(z)\right]^{-n} \quad \text{for} \quad (5.10)$$

$Ri(z) < 1.0$

$$L_m = 0.4z\ (1 - \frac{z}{d})^{\frac{1}{2}}\ (1+\beta)^{-n} \text{ for} \qquad (5.11)$$

$Ri(z) > 1.0$

5. If there is a significant peak in the Ri value at $z = z_i$ and z_i/d is less than 0.75, the momentum mixing length has a constant value given by:

$$l_m(z) = 0.4z_i\ (1 - \frac{z_i}{d})^{\frac{1}{2}}\ [1 + \beta\ Ri\ (z_i)]^{-n} \qquad (5.12)$$

for $Ri\ (z_i) < 1.0$

$$l_m(z) = 0.4z_i\ (1 - \frac{z_i}{d})^{\frac{1}{2}}\ (1 + \beta)^{-n} \qquad (5.13)$$

for $Ri\ (z_i) > 1.0$

except near the bed and the surface where $l_m(z_i)$ is $> l_{mo}(z)$, the homogeneous mixing length and

$$l_m(z) = l_{mo}(z) = 0.4z\ (1 - \frac{z}{d})^{\frac{1}{2}} \qquad (5.14)$$

is applied.

6. The solute mixing length distribution in stratified conditions is

$$l_c(z) = l_m(z)\ \frac{1 - \frac{l_c(z)}{l_m(z)}\frac{Ri(z)}{Rf_c}}{\left[1 - \frac{l_c(z)}{l_m(z)}Ri(z)\right]^2} \qquad (5.15)$$

6 BOUNDARY CONDITIONS

The model was designed for complex estuaries and can accept several types of seaward or landward boundary conditions: either a discharge or level and prescribed concentrations at the landward boundaries and tidal variations in level and concentration

profiles at the seaward boundaries. At the seaward boundary the concentration is found using a characteristic method on the ebb tide and a ramp function is used to determine concentrations during the transition from ebb to flood tide if no prescribed concentration profile is imposed. On the flood tide these concentrations are prescribed. In addition, the convective inertia term is set to zero at the seaward boundary as well as at all the junctions. In the surface layer the equation describing conservation of mass is integrated from the surface layer interface to the surface and becomes:

$$\frac{\delta A}{\delta t} + \frac{\delta \bar{u} A}{\delta x} - WB = 0 \qquad (6.1)$$

Since the model also describes mud transport and allows the bed level to vary, a similar continuity equation should apply to the bed layer. However, because the time scale for significant bed level movement is much greater than the model timestep, the following simplified continuity equation was used for water movements in the bed layer.

$$\frac{\delta u A}{\delta x} + WB = 0 \qquad (6.2)$$

In two-dimensional reaches, the shear stress at the bed is introduced by using a roughness length k_s and by assuming a logarithmic profile in the bed layer. The layer average velocity at the bed is therefore related to the bed stress by the Colebrook-White transition law:

$$\bar{u} = \frac{U_*}{k_s} \ln \left(\frac{e}{Z_B} \left(\frac{k_s}{30.2} + \frac{0.1\nu}{U_*}\right)\right) \qquad (6.3)$$

where ν is the kinematic viscosity of water (m^2/s)

7 NUMERICAL SOLUTION TECHNIQUE

The flow and conservation equations are solved using an implicit finite difference technique using a vertical horizontal rectangular grid set along the centre line of the tidal channel. The main body of water in the channel is thereby divided into a number of thin layers of constant thickness but variable width.

The finite difference grid used in the model is shown in Figure 5. The basic grid is rectangular with velocity components defined at the centre of each face of each grid cell and salinity and suspended solids

concentration defined at the centre of each cell. The horizontal interval (Δx) is variable and is much greater than the vertical interval (Δz) which is constant except in the bed and surface layers. The surface is, at the present state of development of the model, contained within one layer of variable depth and the bed is allowed to move through the grid as as erosion of deposition occurs. The bed layer is allowed to vary in thickness between Δz and $2\Delta z$ and the bed only changes layers when it exceeds these limits. In this way, it is possible to represent the longitudinal bed profile quite accurately. Equations 4.1 to 4.5 are integrated over the depth of each layer and the resulting differential equations and their finite difference representation are derived as follows:-

7.1 Layer averaged equations of motion

Integration of equation (4.1) over the thickness of a layer gives:

$$\frac{\delta \bar{u}A}{\delta t} + \frac{\delta \bar{u}^2 A}{\delta x} + (WuB)_{ku} - (WuB)_{kD} + \frac{A\,\delta P}{\rho \delta x}$$

$$= \left(\frac{\tau B}{\rho}\right)_{ku} - \left(\frac{\tau B}{\rho}\right)_{k} - \frac{f|\bar{u}_k|\bar{u}_k|R}{8} \qquad (7.1)$$

where the side friction term has been included and R is the wetted perimeter.

Similarly integration of equations 4.3, 4.4 and 4.5 yield:

$$\frac{\delta \bar{u}A}{\delta x} + (WB)_{ku} - WB_{kD} = 0 \qquad (7.2)$$

$$\frac{\delta cA}{\delta t} + \frac{\delta \bar{u}cA}{\delta x} + ((W-\omega)cB)_{ku} - ((W-\omega)cB)_{kD} - \frac{\delta}{\delta x}\left(AD\frac{\delta c}{\delta x}\right)$$

$$= (F_c B)_{ku} - (F_c B)_{kD} + \frac{dm}{dt} \qquad (7.3)$$

$$\frac{\delta SA}{\delta t} + \frac{\delta \bar{u}SA}{\delta x} + (WSB)_{ku} - (WSB)_{kD} - \frac{\delta}{\delta x}\left(AD\frac{\delta s}{\delta x}\right)$$

$$= (F_s B)_{ku} - (F_s B)_{kD} \qquad (7.4)$$

The pressure term in any layer can be written in terms of the pressure term in the overlaying layers as (Ref 3).

$$\frac{1}{\rho_k}\frac{\delta P}{\delta x} = \frac{1}{\rho_k}\left(\frac{\delta P}{\delta x}\right)_{ku} + \frac{g}{2\rho_k}\left\{\Delta z\ \frac{\delta \rho}{\delta x}\right)_{ku} + \left(\Delta z\ \frac{\delta \rho}{\delta x}\right)_k\right\} \qquad (7.5)$$

where at the surface

$$\frac{1}{\rho_s}\frac{\delta P_s}{\delta x} = g\ \frac{\delta h}{\delta x} + \frac{\Delta z_s}{2\rho_s}\ g\ \frac{\delta \rho_s}{\delta x} \qquad (7.6)$$

7.2 Finite difference representation

The model uses a six point implicity finite difference scheme of the Crank-Nicolson type for the calculation of $\bar{u}$, h, s and c. W is calculated from equation (7.2) explicitly after the longitudinal velocity has been found. The main terms used in the finite difference equation for the conservation of momentum are:

$$\frac{\delta \bar{u}A}{\delta t} = \left(\frac{\overline{u_k^+} - \overline{u_k^-}}{\Delta T}\right) A_k \qquad (7.7)$$

$$\frac{\delta u^2 A}{\delta x} = A_k \overline{u_k^+}\left(\frac{\overline{u_{k+1}^-} - \overline{u_{k-1}^-}}{2\Delta x}\right) + \frac{\overline{u_k^+}\left(A\overline{u_{k+1}^-} - A\overline{u_{k-1}^-}\right)}{2\Delta x} \qquad (7.8)$$

$$(UWB)_k = \tfrac{1}{4}\left(\overline{u_k^+} + \overline{u_{kD}^+}\right)\left(W_k \bar{B}_k + W_{k+1}\bar{B}_{k+1}\right) \qquad (7.9)$$

$$\text{where } \bar{B}_k = (B_k + B_{k-1})/2 \qquad (7.10)$$

$$\frac{(\tau)}{\rho}_k = \frac{(\ell_k + \ell_{k+1})^2 \left|\overline{u_{ku}^-} - \overline{u_{kD}^-}\right| \left(\overline{u_k^+} - \overline{u_{kD}^+}\right)}{4\Delta z^2} \qquad (7.11)$$

$$\frac{1}{\rho}\frac{\delta P}{\delta x} = g\ \frac{p_s}{p_k}\ \frac{\delta h}{\delta x} + \bar{P} \qquad (7.12)$$

where $P = \sum \Delta z\ \frac{\delta \bar{P}}{\delta x} + g\frac{\Delta z}{2\rho_k}\frac{\delta \bar{P}}{\delta x}k$ from 7.5 and 7.6

$$= g \frac{\rho s}{\rho k} \frac{(h^+_{i+1} + h^-_{i+1} - h^+_i - h^-_i)}{} + P^- \qquad (7.13)$$

$$|U_k|U_k = |U^-_k|U^+_k$$

The above equations have been written for uniform Δx for simplicity. The modification for variable Δx is straightforward and is used in the model. Substituting these terms into equation 7.2 and grouping terms at the new time level gives

$$f^-_{kD}U^+_{kD} + f^-_k U^+_k + f^-_{ku}U^+_{ku} + g^-_k(h^+_{i+1} - h^+_i) = E^-_k \qquad (7.14)$$

where the coefficients f^-_{kd}, f^-_k, f^-_{ku}, g^-_k, and E^-_k are functions of known values of the variables.

$$\text{Setting } U^*_k = U^+_k + g^-_k (h^+_{i+1} - h^+_i) \qquad (7.15)$$

and substituting in 7.14 gives

$$f^-_{kD}U^*_{kD} + f^-_k U^*_k + f^-_{ku}U^*_{ku} = E^- + 0(\Delta T^2) \qquad (7.16)$$

where E- is a function of known variables.

At the bed and surface this equation becomes respectively

$$f^-_k U^*_k + f^-_{ku}U^*_{ku} = E^- \qquad (7.17)$$

$$f^-_{kD}U^*_{kD} + f^-_k U^*_k = E^- \qquad (7.18)$$

Equations 7.16 to 7.18 can be solved in each vertical for U^*_k. The implicit calculation in the vertical direction for U^*_k with horizontal derivative $(\frac{\delta U}{\delta x})$ represented explicitly leads to a stability constraint of the form

$$\Delta T < \frac{\Delta x}{|U|} \qquad (7.19)$$

Having found U_k^*, the variable Q_i^* is introduced where

$$Q_i^* = \sum U_k^* A_k^- = \sum U_k^+ A^- + \sum g_k^- A_k (h_{i+1}^+ - h_i^+) \qquad (7.20)$$

$$\text{ie} \quad Q_i^* = Q_i^+ + A_i^- h_{i+1}^+ - B_i^- h_i^+ \qquad (7.21)$$

where A_i and B_i are known constants. In bulk flow reaches, a similar finite difference representation of the continuity and momentum equations can be written as

$$\mu_i^- = Q_i^+ - \nu Q_{i-1}^+ + \alpha h_i^+ \qquad (7.22)$$

$$f_i^- = Q_i^+ + \gamma h_{i+1}^+ - \phi h_i^+ \qquad (7.23)$$

where μ_i, f_i, ν, α, γ and ϕ are known functions of the variable at the previous timestep. Equations 7.21, 7.22 and 7.23 can now be solved to determine all Q_i^+ and h_i^+ throughout the model. U_k^+ can then be determined from 7.15 and w_k^+ from 7.2.

Having determined the flow field, the equations for the conservation of salt and mud can then be solved using the ADI method detailed below for the salt equation:

$$\frac{s^* A^* - s^- A^-}{\Delta T/2} + \frac{1}{2\Delta x}\left((s_{k+1}^- + s_k^-) - u_k^- A_k^- (s_{k-1}^- + s_k^-)\right) x$$

$$u_{k-1}^- A_{k-1}) + \frac{1}{2}\left((s_{ku}^* + s_k^*)\, w_{ku}^* B_{ku} - (s_k^* + s_{ku}^*)\, w_k^* B_k\right)$$

$$- \frac{D_k A_k}{\Delta x^2}(s_{k+1}^- - s_k^-) + \frac{D_{k-1} A_{k-1}}{\Delta x^2}(s_k^- - s_{k-1}^-)$$

$$= B_{ku}\, lm_{ku}\, lc_{ku} \left| u_{ku}^* + u_{ku-1}^* - u_k^* - u_{k-1}^* \right| x$$

$$(s_{ku}^* - s_k^*)/2\Delta z^2 - B_k\, lm_k\, lc_k \left| u_{k-1}^* - u_{kD}^* \right| (s_k^* - s_{kD}^*)/2\Delta z^2$$

$$\text{where} \quad W_k^* = (w_k^+ + w_k^-)/2 \qquad (7.24)$$

$$U_k^{*1} = (u_k^+ + u_k^-)/2$$

$$\frac{s^+A^+ - s^*A^*}{\Delta T/2} + \frac{1}{2\Delta x}\left((s^+_{k+1} + s^+_k)u^+_k A_k - (s^+_{k-1} + s^+_k)\right) x$$

$$u^*_{k-1}A_{k-1}) + \frac{1}{2}\left((s^*_{ku} + s^*_k)w_{ku}B_{ku} - (s^*_k + s^*_{kD})\right) x$$

$$w^*_{kD}B_{kD}) - \frac{D_k A_k}{\Delta x^2}(s^+_{k+1} - s^+_k) + \frac{D_{k-1}A_{k-1}}{\Delta x^2}(s^+_k - s^+_{k-1})$$

$$= B_{ku}lm_{ku}lc_k\left|u^*_{ku} + u^*_{ku-1} - u^*_k - u^*_{k-1}\right| x \qquad (7.25)$$

$$(s^*_{ku} - s^*_k)/2\Delta z^2 - B_k lm_k lc_k\left|u^*_k + u^*_{k-1} - u^*_{kD}\right)/2\Delta z^2$$

8 PHYSIO-CHEMICAL PROPERTIES OF MUD

HR have investigated the rheological properties of many marine muds as part of basic and ad hoc engineering studies. Mud consists of a mixture of clay particles (less than 2 μ), silt (less than 60 μ) and sand. Flocculated clay particles form a bulky, cohesive matrix which contains small, non-cohesive particles of silt and fine sand. The main effect of the sand and silt content is to increase the bulk density of a settled mud deposit. Tidal mixing processes tend to even out variations in the physio-chemical properties of the clay fraction in an estuary. The settling velocity of individual clay particles in fresh (non-saline) river water is assumed to be negligible. Flocculation is usually complete when the salinity exceeds about 0.5ppt.

9 SETTLING VELOCITY OF MUD FLOCS

The settling velocity of mud flocs in suspension in the saline regions of estuaries can be determined using an Owen settling tube and HR have made such observations in many estuaries over a period of years. It has been found that the settling velocity of flocs in natural tidal waters, for concentrations in the range 0-4000ppm, are generally about an order of magnitude higher than those determined in the laboratory. The much higher settling velocities in the field are assumed to be caused by the much longer flocculation time and different turbulent characteristics in natural flows. The size and hence

the settling velocity, of mud flocs has been shown to be a strong function of the concentration of suspended solids. The settling velocity of flocs is determined by the balance between their submerged weight and the viscous drag, as represented by Stoke's Law. Their settling velocity is therefore influenced by the water temperature. It seems unlikely that salinities in excess of 0.5ppt have any influence on the settling velocity of flocs other than causing a change in their submerged weight. Existing data has been analysed for its dependency on concentration of suspended solids and this shows that the median settling velocity is a relatively well defined function of the concentration. For concentrations in the range 0-4000ppm, the settling velocities increase with about the four-thirds power of the concentration. The scatter in this region is thought to arise mainly from differences in the local rate of dissipation of turbulent energy. The median settling velocity reaches a peak and remains constant at about 2mm/s for concentrations in the range 4000-20000ppm. In this range of concentrations the particles are beginning to hinder each other settling. The settling velocity of mud flocs in the range of concentrations higher than 20,000ppm decreases rapidly and reaches a minimum value of about 0.05mm/s for fluid mud with concentrations of about 75,000ppm.

The flux of settling particles, which is the product of the settling velocity and the concentration, reaches a peak value for concentrations of about 20,000ppm. The vertical distribution of suspended mud depends on the changing balance between the downward flux of settling particles, and the upward flux due to vertical turbulent exchange. The form of the relationship between the settling velocity and the concentration plays an important role in determining the rate of deposition of mud and the formation of fluid mud at slack water. Mud will deposit from flowing water if the bed stress is less than about $0.1 N/m^2$. If the suspension in the lowest layer has not reached the concentrations of fluid mud, it will settle at the following rate:

$$\frac{dm}{dt} = \omega c \left(1 - \frac{\tau_b}{0.1}\right) \text{ kg/m}^2\text{/s} \qquad (9.1)$$

where ω = function (c).

10 FORMATION OF A MUD DEPOSIT

Provided the concentration of the suspended solids in the overlying water is less than about 2,500ppm, which is a common situation in many estuaries, the mud will settle directly on the bed and form a deposit in which

the density and shear strength increases rapidly with depth. The main body of a mud deposit, which is not usually disturbed during a normal tidal cycle, has a much higher and more uniform density and shear strength. The thin surface layers, which are only a few millimetres thick, are often called 'slack water deposits'. This is because they are usually re-eroded as soon as the tidal currents increase after the turn of the tide. The slack water deposit also usually forms after any sand has settled onto the bed.

Rheological and flume experiments indicate that the shear strength of a mud deposit increases with the 5/2 power of the concentration (dry weight per unit volume).

$$\tau_e = k\ \gamma_D^{5/2}\ (N/m^2),\ \text{for}\ \gamma_D > 75 kg/m^3. \qquad (10.1)$$

In fact, the structure of the matrix of mud flocs is such that the density increases in sudden steps as aggregations of one floc size and density collapses to the next smaller and stronger grouping. It is assumed that the water takes hardly any time to drain vertically through the very thin overlying aggregation of mud flocs.

For the mathematical model, laboratory data may be used to find the mean density and mean shear strength of a number of idealised sub-layers in the bed and in the present model, four layers are used which are assumed to contain a constant mass of dry matter per unit area of bed. For example, the density, shear strength and corresponding thickness of the four layers might be as follows:

Layer	Shear Strength N/m^2	Dry Density kg/m^3	Thickness mm	Mass kg/m^2
1	0.1	100	1.60	0.16
2	1.0	175	0.91	0.16
3	2.0	250	0.64	0.16
4	3.0	325	0.49	0.16

The density and strength of the mud matrix in the main body of the bed tends to remain constant with depth for between 0.5-10m, indicating very slow consolidation. This may be explained by the fact that the size of the pathways for water to pass through the mud matrix rapidly decrease with increasing density effectively preventing further consolidation of the sub-surface layers.

The model allows the slack water deposits to form in the following manner: the mud accumulates in layer one until it exceeds 0.16kg/m^2, at which time layer two fills up and 0.16kg is removed from layer one. Layer three fills up when the weight of mud in layers one and two exceeds 0.32kg/m^3 etc. When all four sub-layers are full, the excess mud is added to the main body of the bed which is assumed to have a uniform density and shear strength. The slack water deposit may appear to be very thin but the mass of mud contained in four full layers (0.64kg/m^2) is equivalent to a mean concentration of 64ppm in 10m of water.

11 EROSION AND RESUSPENSION OF MUD

Research by HR has shown that the rate of erosion of the surface of a mud deposit may be calculated in terms of an excess shear (N/m^2) over and above that required to initiate motion, τ_e, which is itself dependent on the dry density of the the exposed surface.

$$\frac{dm_e}{dt} = M_e (\tau_b - \tau_e) \text{ (kg/m}^2\text{/s)} \qquad (11.1)$$

where M_e is an empirical constant.

Observations of the rate of rise of suspended solids concentration near the bed in estuaries after the change of the tide indicate that the sub-layers in the slack water deposit erode almost instantaneously as the tidal velocities increase. So, for the purposes of the model it was assumed that the whole mass of mud in each sub-layer (0.16kg/m^2 in the example quoted) would be eroded as a sheet as soon as the bed stress exceeded the prescribed critical value. The main body of the bed was assumed to erode more steadily according to equation (11.1). The bed stress exerted by the flow on the bed depends on the roughness of the mud surface. This may be smooth ($k_s = 0$) but there is evidence that the effective roughness of an eroding mud bed is in the order of 1 or 2mm. The model logs or records the state of the slack water deposit and automatically fills and empties each layer depending on the rate of erosion or deposition. It is possible, for example, for only three of the slack water sub-layers to be eroded on a neap tide and for two to reform at slack water, leaving the deposit with a missing third layer.

11.1 Sand-mud mixtures

The model simulates the effect of different mixtures of sand and mud in the main body of the bed. The slack water deposit is assumed to be free of sand particles, which settle to the bed early in the slack water period. The composition of the main body of the bed is schematised into four size fractions: three being sand and one being mud. In the model the main body of the bed is divided into a number of relatively thin (200mm) horizons each containing varying amounts of each sediment fraction.

The proportion of the bed surface available for erosion is normally assumed to be related to the volume of each sediment type contained in the exposed horizon. Erosion of the sub-surface horizons cannot take place until all the sediment of whatever size has been eroded from the surface horizon, down to some minimum thickness. This allows a thin layer of coarse sediment or cohesive mud to protect or armour underlying layers of more easily erodible material.

11.2 Sand in suspension

The vertical distributions of suspended mud and sand particles in a tidal flow can normally be considered to be almost independent of each other as regards particle interactions because of the relatively low concentrations. Even the finest sand particles have a settling velocity which exceeds that of most mud flocs. Whereas mud may be uniformly distributed over the vertical, sand concentrations usually increase rapidly near the bed.

At present it is not common practice to calculate the concentrations of sands in suspension in different levels in shallow tidal flows. Instead one calculates the total rate of transport of a given grain size in terms of its availability on the bed, the bed shear stress and water temperature. To date, there are no methods for predicting this saturated rate of sand transport without recourse to one or more empirical relationships based on field data. However, in deep tidal flows it may take a significant amount of time for the finer sand fractions to be lifted into the upper layers of the flow by vertical turbulent exchange. This means that the actual load of sand carried by the flow may be greater or less than the saturated value depending on the availability of sediments in the up-flow direction. Recent research by HR has shown that its possible to take into account some of these unsteady effects without a full solution of the concentration equations. This is done by introducing two extra parameters which take into account the vertical structure of the unsteady velocity and concentration profiles. The details of

the total bed load type of sand transport function used in the model are outside the scope of this report.

12 APPLICATION TO THE BRISBANE RIVER ESTUARY

The first application of TIDEFLOW-2DV was to the Brisbane river estuary in Australia where the Port of Brisbane authority (PBA) is developing new port facilities near the mouth of the Brisbane tidal river. The proposed work in the estuary includes lengthening, deepening and widening the existing swing basin area and deepening the approach channels. PBA also wish to cease or reduce maintenance dredging upstream in the existing port area some 19km from Moreton Bay, Figures (8) and (9).

The main objectives of the investigation were: (i) to identify, quantify and simulate the processes causing siltation in the navigation channels, swing basins and berths in the seaward reaches of the Brisbane river estuary; (ii) to predict the effect of capital dredging works associated with port developments at Fisherman Islands and changes in the patter of maintenance dredging in the existing port area on siltation in the tidal river.

TIDEFLOW-2DV was used to simulate the unsteady patterns of mud transport and siltation resulting from the interaction of tidal flows with short flashy fluvial floods, which are the main cause of shoaling in the port. The dredged channel silts up with muddy sediments at a rate of about 1.5 million cubic meters per annum where the bulk of the siltation is located in the existing port area especially in Hamilton Reach (Fig 9).

The estuary has a typically flashy hydrograph with long periods of practically no flow interspersed with short flood events which usually occur in the months between December and April and last on average about 12 days. The tidal regime in Moreton Bay is a mixed one with significant diurnal and semi-diurnal constituents, the M_2 semi-diurnal tidal constituent being the largest with an amplitude of 0.72m. The tidal compartment of the Brisbane river is narrow compared to its length , which is about 100km from the entrance to Mount Crosby weir.

HR and PBA mounted two identical two-day long intensive simultaneous observations at seven sections between km 4 and km 26 in the port area in the dry season in August 1977, and again during the passage of a small fluvial flood in April 1978. HR also supplied the PBA survey team with a rapid-drop

profiler (RDP) (Ref 5), which was mounted on a fast launch and was used to monitor suspended solids and salinity profiles throughout the length of the estuary at regular intervals.

For economy, the TIDEFLOW-2DV model was designed to simulate only those reaches of the estuary where the vertical structure of the flow was thought to be important. The other reaches where the flow was vertically well mixed was simulated in one dimension. In the case of the Brisbane estuary, the seaward 40km was simulated in two dimensions with layers 1m thick. The remaining landward portion of the estuary was simulated in one dimension. A schematic representation of the elements in-plan is shown in Figure (11).

A study was made of the geology and recent sedimentology of the estuary with the aim of finding the distribution of bed surface sediment types. A variety of historical data was examined including a mixture of seismic data, drilling logs, grab sampling analyses and side sonar plots. The historical data was supplemented by a series of new field investigations undertaken by HR and PBA in the surface 1 or 2m of the river bed. This included collection of bed surface grab samples, vibro core samples, and bulk density profiles using a radioactive transmission probe. The main findings of this investigation were that the sediments below the project dredged depth were generally inerodible rock, gravel or clay. The main silting material in the port area is a slightly sandy mud with the following average properties:

Total bulk density - 1.3 tonnes/m^3
Total dry density - 0.5 tonnes/m^3
Sand fraction (60 - 150 microns) about 25% by weight
Bulk density of mud matrix - 1.25 tonnes/m^3

In the model, the tidal level at the mouth of the estuary was synthesised using the diurnal, semi-diurnal and quarter diurnal harmonic constants (Fig 10). The model also required a seaward boundary value for the salinity and suspended solids concentrations on the incoming tide. These were prescribed from field data.

13 SUSPENDED MUD LOAD OF THE RIVER

HR made an analysis of the discharge and suspended sediment records of the Brisbane and Bremer rivers with the aim of determining the frequency and distribution of fluvial flows and the quantities of suspended sediments brought into the estuary. The analyses show that the river has a typically flashy hydrograph with long periods of practically no flow

interspersed with short flood events, which usually occur in the months between December and April. An approximate correlation was established between the mean daily discharge and the suspended mud load of the rivers. The optimum value for the constant of proportionality for the Brisbane river sediment rating function was established by equating the total sum of synthesised sediment loads for a number of flood events with the total observed load for all the events. The mud concentration in the river was found to vary approximately linearly with the discharge. The analyses show that the annual influx of mud into the head of the estuary varied from about 30,000 tonnes in 1975 to over 5 million tonnes in 1974. It is estimated that on average about 600,000 tonnes of mud enters the estuary every year from the rivers.

14 SIMULATION OF CONDITIONS DURING THE DRY SEASONS

Initially, the model was set up to simulate a repeating 25 hour spring tide cycle during the dry season. Results from the model were compared with observations made during the simultaneous exercise in August 1977, when the fluvial flows had been very low for several months. There was still a significant salinity gradient in the estuary, but there was some difficulty in defining the longitudinal salinity distribution because the field observations were suspect. However, the model simulated the correct pattern of tidal propagation (Figure 13) and the main features of the vertical structure of the tidal currents in the port area, Figures (14) and (15). It should be noted that the results from the model refer to laterally averaged values, whereas the observations were measured at a single vertical in the middle of the channel.

The small degree of stratification and the weak longitudinal density gradients affect the velocity profiles and time histories in the following manner. The stratification delinks the surface and sub-surface layers allowing them to move relatively independently of each other. The longitudinal density gradient generates a small but steady landward force on the water in the lower layers. This causes the currents to start to flood in the bed layer almost two hours before the surface layer. There is a strong bias in the landward direction in the bed layer and an equally strong bias in the seaward direction in the surface layers. The residual velocities generate a two-layer gravitational circulation.

The model also simulated the main features of the pattern of mud transport and siltation in the dry season, Figures (16) to (17). The suspended

concentrations were rather low in the range 20-40ppm in the port area. Hardly any deposition occurred at slack water due to the very low settling velocities. Note that the observations were made at a point whereas the model values are averaged both across the channel and along a 1,000m long element. An analysis of the model results in terms of tide averaged mud concentrations and near bed salinities show how the salinity distribution determines the location of maximum turbidity, which was about 20km upstream of the port, Figure (17). The analysis showed that the longitudinal distribution of siltation is governed both by the turbidity and the duration of periods when deposition can occur during the tidal cycle, Figure (18). The model showed that there were two zones of siltation in the dry season, one near the toe of the saline intrusion (km 35-45) and a second one just upstream of the port area (km 20-30).

15 SIMULATION OF CONDITIONS DURING AND IMMEDIATELY AFTER A FLUVIAL FLOOD

The model was then used to simulate the passage of a small fluvial flood which was observed in April 1978 after a long period of low fluvial flows. Such fluvial floods are considered to be the main cause of siltation in the port. The interaction of the tide and the fluvial flows result in a very unsteady pattern of saline intrusion and sediment transport which is unique to each flood event and which can only be simulated in a model representing the vertical structure of the flow.

The observed flood, which on average is exceeded about three times a year, occurred in two stages after a long period of negligible fluvial flows Figure (19). During the first phase, the river discharge rose to a value of about $40m^3/s$ for about 10 days. The main flood started on the 2nd April and peaked on the 3rd April. RDP surveys were made on the 4th, 5th, 6th and 7th April 1978. A standard type of simultaneous survey at several fixed stations was made in the port area on the 10th and 11th April 1978.

The initial conditions for the model simulation were set approximately using the results from an RDP survey on 29th March 1978. The salinity of the incoming sea water at the mouth of the estuary was set to remain constant at 30ppt, which was lower than the value observed on the 29th March 1978 (which may have been erroneous) but similar to the values recorded on all the later surveys. The model was run from 29th March to 12th April 1978.

An approximate comparison between the predicted and observed longitudinal profiles of salinity and turbidity in the bed and surface layers on the main run of the flood and ebb tides on the 4th and 7th April 1978 are shown in Figures (20) and (21). The multi-layer reach only extended to km 40; beyond this section the model was one-dimensional. It should be noted that the RDP profiles were not simultaneous and the observations were made at random verticals somewhere in the centre of the estuary. The model values are averaged over a thickness of 1m, the width of the estuary and along a 1,000 reach.

The model appears to reproduce the main features of the very unsteady processes adequately considering the large number of assumptions made in the calculation. For example, the concentration of mud in the river was based on a rating function and the salinity on the incoming tide in the mouth of the estuary was set to be a constant. The degree of vertical stratification in the Hamilton Reach rose to a peak value of about 20ppt on the 4th April at the height of the flood, Figure (22). The model was more accurate at simulating the depression of the surface salinity than the bed salinity, which was strongly influenced by the prescribed seaward boundary value of 30ppt. The model predicted the location of the peak in suspended solids concentrations in the bed layers as it moved down the estuary, but tended to under-estimate the observed values in the centre of the channel.

The unsteady fluvial flows generated an equally unsteady gravitational circulation, which persisted long after the fluvial flood flows had dropped. The steep longitudinal density gradients produced a strong landward bias in the velocities in the bed layer in the port area, Figure (23). The predicted pattern of deposition and erosion in Hamilton Reach (km 19) is illustrated in Figure (24). This shows that there is no sudden peak in siltation coinsiding with a peak in the fluvial flow. This probably did not happen because the flood did not bring down much new sediment into the estuary. Its main effect was to strengthen the gravitational circulation which carried more sediment into the estuary from Moreton Bay. A schematic representation of the sedimentation process is shown in Figure (25). An analysis of the model results show that during the 10 day period of the flood, 8,000 tonnes of fluvial mud entered the head of the estuary and 10,000 tonnes of marine mud entered the mouth of the estuary.

It takes a considerably longer time for the mud to reach the lower estuary than for the fluvial water to be evacuated from the estuary. This occurs because a considerable fraction of the new sediment is

periodically re-suspended and carried back up the estuary in the lower layers on the flood tide whereas the fluvial water passes fairly rapidly out of the estuary via the surface layers without greatly affecting the longitudinal salinity distribution in the lower layers of the flow. Each fluvial flood carries an extra load of mud into the estuary and uniquely and temporarily alters the pattern of tidal propagation, saline intrusion and sediment transport for a period of several weeks. The suspended sediment moves progressively seaward on each tidal cycle until it becomes flocculated by the sea water, periodically eroded, transported and deposited by the tides, and translated by the gravitational circulation until it settles in the deep dredged reaches of the lower estuary where the currents are no longer strong enough to resuspend it. The rate and pattern of siltation in any one wet season depends on the frequency, magnitude, duration and sediment load carried by each fluvial flood and the manner in which it interacts with the tidal flows. It seems very likely that the sediment brought into the estuary during fluvial floods is re-worked and eventually deposited in the deep dredged areas several months after the flood event.

16 TRAPPING EFFICIENCY OF THE ESTUARY

The trapping efficiency of the estuary and the location and longitudinal distribution of siltation is a function of the volume of each individual fluvial flood and the artificial geometry of the lower estuary imposed by capital and maintenance dredging works. For practical purposes, one can assume that most floods in the Brisbane river have a duration of about 12 days and that the volume of flood water is approximately proportional to the peak discharge, Table 1, Figure (26). The mud load of a flood on the other hand increases approximately with the square of the peak discharge. Observations and mathematical model calculations show that almost the entire sediment load of small and medium floods is trapped within the estuary with little loss to Moreton Bay. The effect of the larger floods is to push the centre of gravity of siltation further seaward and to spread the zone of siltation over a longer reach. At some critical flood stage, depending on the depth of the estuary, the fluvial discharge is big enough to flush the saline wedge out of the estuary: which allows a large proportion of the mud load brought down by the flood to pass out of the estuary. The flood causing the worst amount of siltation is therefore not the largest one. For example, the 1974 flood caused little damage to the port in terms of mud siltation. A consideration of the frequency of given flood events

shows that there is some smaller flood which on average causes the most damage to the port. The model was used to calculate the trapping efficiency of the estuary for a range of flood magnitudes.

17 ANALYSIS OF FLOOD DATA 1927-1972

Data on all daily fluvial flows in excess of 10 cumecs over Mount Crosby weir from 1927 to 1972 was made available by PBA. This data comprised 414 flood events in the 46 year period covered by the data giving, on average, 9 floods per year. The flood hydrographs have approximately the same shape and 10 day duration regardless of peak discharge, as illustrated in Figure (26). The floods were divided into classes, according to volume, each class covering a range of 25 million m^3 and the average flood volume in each class was calculated. Table (1) shows the results of this classification. Figure (27) shows the frequency of flood events as a function of the total volume passing over Mount Crosby weir.

The model was used to predict the trapping efficiency of the estuary for four different floods, numbered 1 to 4 in order of decreasing size, which were considered to be representative of the whole range of historical flood events, excluding the 1974 '100 year flood'. The fluvial flow was specified as a series of mean daily discharges. The model assumed a linear variation between daily values in order to obtain a continuous hydrograph and the suspended sediment concentration was obtained from the discharge using empirical relationships for the Brisbane and Bremer rivers. The initial distributions of salt and suspended sediment were set to be representative of conditions at the end of a period of low fluvial flows. These initial values were not considered to have a significant effect on the results except perhaps in the case of the smallest floods because conditions in the estuary responded rapidly to the fluvial discharge.

The model also required the specification of an initial distribution of bed sediment types. This was essential - especially in the upper estuary - in order to present the model with the appropriate distribution of bed sediment which could, if conditions permitted, be eroded and re-deposited in the lower reaches of the estuary.

All the model simulations assumed that the concentrations of salinity and suspended sediment in water entering the estuary from Moreton Bay in the lower layers would be constant at 30ppt and 30ppm respectively. In reality, these values would vary depending on the particular flood event and the rate

of mixing of fluvial and tidal waters in Moreton Bay. However, it was thought that the values were appropriate for the two small floods. For the two larger floods there was a large net discharge of sediment into Moreton Bay and it was considered that the suspended sediment boundary value was not so important.

17.1 Results

The mass balance of deposition, erosion and mud transport predicted by the model is summarised in Table (2) for each flood event and the predicted longitudinal distributions of mud siltation for each of the tests is shown in Figures (28) to (31).

17.2 Flood 1

The largest of the floods with the return period of 5 years caused a significant amount of erosion in the upper reaches with the smallest amount of deposition landward of km 23.5 of any of the floods. There was only a small amount of deposition in Hamilton Reach, (km 20-23.5) compared to the total influx of sediment and, as can be seen from Table (2), a smaller amount of deposition than that resulting from flood 2. In the lower estuary: seaward of km 20, this flood deposited the lowest percentage (40%) of the total influx of sediment of any flood, but this was still more than double that deposited by flood 2 and amounted to a total of 272,000 tonnes. Perhaps the most significant feature of this flood was that it discharged 70% (421,000 tonnes) of the total fluvial sediment load into Moreton Bay. Most of the deposition in the estuary occurred over a period of three days as shown in Figure (28).

17.3 Flood 2

The sediment load of this flood, which has a return period of 3 years, is approximately 30% of that of flood 1. Total deposition for this flood, however, was proportionally greater with an equivalent of 88% of the fluvial influx being trapped in the lower estuary. This is equivalent to 60% of that deposited by the much larger flood 1. The pattern of deposition for this flood, Figure (29), was quite different to that for flood 1, Figure (28), with a much larger percentage being deposited above km 10.

17.4 Floods 3 and 4

These two floods have return periods of once and three times per year on average. Both floods resulted in a comparatively small amount of net erosion in the upper reaches. The fresh water flows, however, generated gravitational circulations resulting in a net influx of sediment from Moreton Bay. Flood 3 resulted in the majority of the sediment being deposited in an upstream of Hamilton Reach at km 19 Figure (30). The

net influx of sediment plus the change in suspended load between the start and the end of the test represented 25% of the total deposition. Flood 4 also deposited the major fraction of the sediment in and above Hamilton Reach, Figure (31). In this test, the net influx of sediment plus the change in suspended load accounted for 70% of the total deposition, Table (2).

18 TRENDS IN THE MODEL PREDICTIONS

The model showed that large infrequent floods result in a large amount of deposition in the lower reaches of the estuary with a much smaller amount of deposition in and above Hamilton Reach. The large floods discharge the majority of their load into Moreton Bay. The trapping efficiency of the estuary (ie the net amount of mud accumulating in the estuary as a percentage of the fluvial load) as a function of the volume of flood water passing over Mount Crosby weir is shown in Figure (32).

The smaller more frequent floods deposit most of their sediment load in the upper reaches of the estuary and generate a gravitational circulation which could carry a significant mass of mud from Moreton Bay into the estuary. The region over which this marine mud is deposited will depend on the position of the limit of saline intrusion which will vary depending on the fluvial discharge. For small floods the limit of saline intrusion was always found upstream of Hamilton Reach km 19. For the larger floods, the limit of saline intrusion was pushed well downstream of Hamilton Reach - before moving back upstream as the fluvial flood subsided - with the resulting different pattern of siltation. The large floods, of course, also generate a gravitational circulation but the mass of sediment involved in this circulation is small compared to the total influx of river sediment. It was found that, by continuing the simulation of floods 1 and 4 after the fluvial flows had subsided that about 1,000 tonnes per day entered the estuary from Moreton Bay and that the bulk of this sediment was deposited at Hamilton Reach.

The process of re-working sediment deposited in the lower estuary by the residual gravitational circulation following a flood may be important. This process would be most significant following a major flood when some of the large mass of sediment initially deposited in the lower estuary would in time be eroded and re-deposited in the more landward reaches. The final distribution of siltation would therefore vary with time after the initial rapid deposition had finished.

19 LONG TERM AVERAGE ANNUAL RATE OF SILTATION

The long term average rate of siltation between 1927 and 1972 was estimated by evaluating the net movement of mud into the estuary for each class of flood by interpolation and extrapolation from Figure (33) and multiplying it by the recorded number of floods in each class (column 2 in Table (3)) and summing the total. This method gave a total mass of siltation of 11,400,000 tonnes for the 46 year period which is equivalent to a long term rate of 250,000 tonnes per annum. This is equivalent to an annual in-situ volume of about 600,000m^3 (assuming a bed dry density of 0.4 tonnes/m^3).

In addition, the model predicted a continuing rate of siltation of approximately 1000 tonnes/day in and downstream of Hamilton Reach following each flood event. This deposition is likely to persist for at least 20 days after the passage of a flood of any magnitude, and since there are on average 9 floods per year, the additional influx of mud could amount to 180,000 tonnes/year with an in-situ volume of 450,000m^3. This figure is only approximate and will depend on the concentration of suspended sediment in Moreton Bay which in turn will depend on any preceeding floods. However, this additional influx of mud from Moreton Bay will bring the total predicted average annual siltation rate in the order of 1 million m^3 which compares approximately with the long term average recorded rate of dredging measuring by hopper volume.

An analysis of the model results show that floods with a return period greater than 1 in 5 years only account for about 13% of the total siltation, whereas the three smallest classes of flood account for 42% of the total siltation, most of which occurs in the upper reaches of the port.

20 CONCLUSIONS

During the past decade, there has been a steady improvement in the understanding and theoretical description of mud transport processes in tidal channels. This has made it possible to construct general purpose mathematical models, which can simulate the main features of the complete cycle of processes which determine the pattern of siltation in a narrow estuary. In the author's opinion, the practical application of the technique has now reached a stage where it can be employed as an almost standard procedure for investigating and solving siltation problems in narrow estuaries.

A viable mathematical model requires sets of equations to describe the processes represented in the model, which should be based on well grounded physical concepts , theory and experiments. Certain aspects of the processes of mixing, energy dissipation and sediment transport, as yet, can only be defined by semi-empirical relationships based on field observations and laboratory experiments. The physical equations and functional relationships determine the structure of the model but the results depend heavily on the values of the constants and engineering coefficients applied to a particular situation. A viable model from the point of view of engineering applications requries an efficient, reliable and accurate method of solution of the equations, giving due regard to the quality of the data and the accuracy required from any predicted calculation. HR employ implicit 6 point finite difference schemes with second order accuracy and a timestep varying between 5 and 10 minutes depending on the particular application of the model. Such a short timestep is required to resolve the rapidly varying flows and conditions for scour and deposition that occur at the bed of an estuary at certain stages of the tidal cycle.

A model of mud transport in an estuary requires boundary conditions in terms of water levels, salinities and suspended solids on the incoming tide at the seaward boundary and the fluvial discharge and suspended concentrations at the landward boundaries. Models require a mass of bathymetric and sediment data to define the geometry and the distribution and grading of sediments in and along the bed of the estuary. A second mass of field data in terms of water levels, velocities, salinities and suspended solids is required to prove and validate the model for a range of tidal and fluvial conditions.

The two-dimensional in-depth model TIDEFLOW-2DV, described in this report, is considered to be a "state of the art" model.

Port works often involve construction of dredged entrances and turning basins which can give rise to sudden expansions in an otherwise narrow channel. At present, this problem is usually handled by undertaking a physical model or a separate calculation with a two-dimension in plan mathematical model to calculate the distribution of siltation across the channel. Ideally, one would wish to connect the channel model described in this report with a local three-dimensional numerical model. However, as yet, a suitable three-dimensional mud transport model has not been developed, nor do the present generation of computers have the capacity to run 2 and 3-dimensional

models simultaneously. Hydraulics Research hope to overcome both these problems in the next few years.

21 ACKNOWLEDGEMENTS

HR gratefully acknowledge the helpful co-operation of the Port of Brisbane Authority in allowing Hydraulics Research to use their estuary at the test bed for developing the model.

22 REFERENCES

1. Odd NVM and Owen MW "A two-layer model of mud transport in the Thames estuary". Proceedings of the Institution of Civil Engineers, London. Supplement ix paper 7517S, 1972, 175-205.

2. Hydraulics Research Station Report EX 883 "Saline intrusion and sediment transport in the Rotterdam waterways. A two-layer numerical model simulation study". 1979.

3. Rodger JG "Simulation of stratified flows in estuaries". 2nd IAHR Symposium on stratified flow, Trondheim 1980.

4. Odd NVM and Rodger JG "Vertical mixing in stratified tidal flows". Proceed ASCE, Hy3, 1978.

5. Odd NVM and Baxter T "Port of Brisbane siltation study". 17th Coastal Engineering Conf., Sydney, 1980.

TABLE 1

STATISTICS OF FLOOD EVENTS SIMULATED IN THE MODEL

	Return period years	Duration of model test days	Combined Brisbane & Bremer river flood volume $m^3 \times 10^6$	Peak discharge Brisbane & Bremer m^3/s	Prescribed sediment load tonnes	Start date
Flood 1	5	11	1000 (666)	3500	600000	7/7/73
Flood 2	3	11	650 (435)	2260	183000	19/1/76
Flood 3	1	9	330 (221)	1080	43500	9/2/76
Flood 4	0.3	11	85 (57)	364	8000	29/3/78

NB Bracketed figures refer to Brisbane River

TABLE 2

MASS BALANCE OF MUD TRANSPORT IN THE ESTUARY

(thousands of tonnes of dry mud)

Flood	Influx of fluvial mud	Net discharge of mud to Moreton Bay	Erosion of upper reaches of estuary	Change in suspended mud in estuary	Gross siltation in estuary	Net siltation in estuary	Net movement of mud into estuary
	(1)	(2)	(3)	(4)=(1)-(2)+(3)-(5)	(5)	(6)=(5)-(3)	(7)=(1)-(2)
1	600	421	81	-12	272	191	179
	100%	70%	14%	2%	45%	32%	20%
2	182	58	34	-3	161	127	124
	100%	32%	19%	2%	88%	70%	68%
3	43	-5*	5	-9	62	57	48
	100%	12%	12%	21%	144%	133%	112%
4	8	-10*	1	-10	29	28	18
	100%	125%	13%	125%	363%	350%	225%

* Net influx of marine mud from Moreton Bay

Percentages refer to value in column (1)

TABLE 3

HINDCAST MUD SILTATION 1927-72

Flood volume range (million m^3) (1)	Number of floods in class (2)	Mean flood volume in class (passing Mound Crosby Weir) (3)	Siltation per flood event (1000's tonnes) (4)	Siltation per class of flood (1000's tonnes (5) = (2)x(4)
1175-1200	1	1200	(100)	(100)
1150-1175	0	0	-	-
1125-1150	0	0	-	-
1100-1125	1	1110	(135)	(135)
1075-1100	0	0	-	-
1050-1075	1	1060	(163)	(163)
1025-1050	0	0	-	-
1000-1025	0	0	-	-
975-1000	1	997	(165)	(165)
950-975	0	0	-	-
925-950	1	939	(176)	(176)
900-925	0	0	-	-
875-900	0	0	-	-
850-875	0	0	-	-
825-850	0	0	-	-
800-825	0	0	-	-
775-800	1	786	(188)	(188)
750-775	0	0	-	-
725-750	1	743	187	187
700-725	1	707	184	184
675-700	0	0	-	-
650-675	1	665	179	179
625-650	0	0	-	-
600-625	0	0	-	-
575-600	1	589	167	167
550-575	0	0	-	-
525-550	0	0	-	-
500-525	3	510	148	444
475-500	0	0	-	-
450-475	0	0	-	-
425-450	1	445	128	128
400-425	7	413	118	826
375-400	0	0	-	-
350-375	2	367	103	206
325-350	4	338	92	368
300-325	5	308	81	405
375-300	4	288	73	292
250-275	1	259	62	62
225-250	5	241	56	280
200-225	3	215	46	138
175-200	4	190	40	160
150-175	10	165	34	340
125-150	14	140	29	406
100-125	17	111	24	408
75-100	22	89	22	484
50-75	44	61	18	792
25-50	71	37	17	1207
0-25	187	11	15	2805

Total siltation (dry tonnes) 11,395,000
over 47 years (m^3) 28,500,000

Notes: Estimated values are bracketed
Dry density 0.4t/m^3

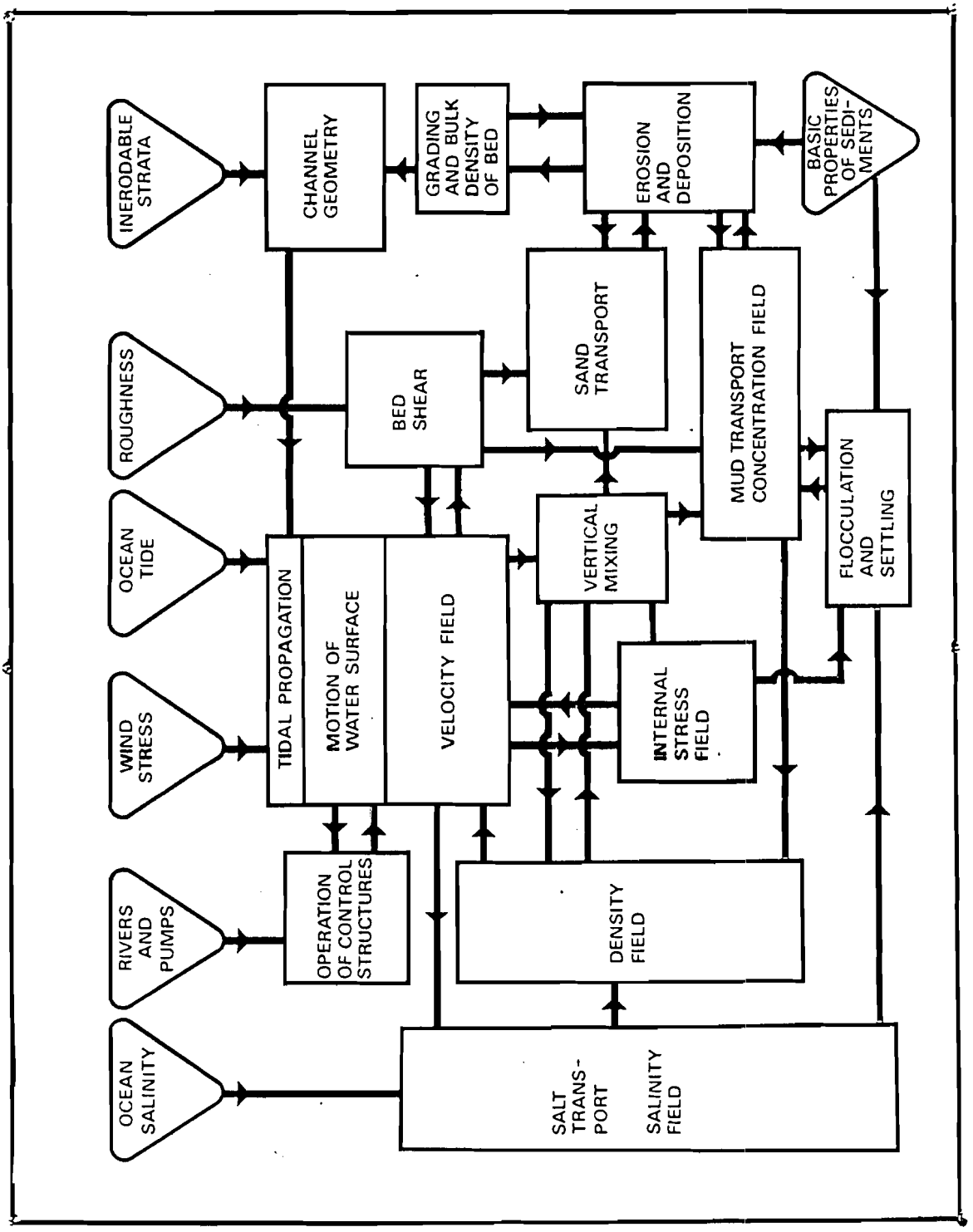

Fig 1 Interaction of tidal processes

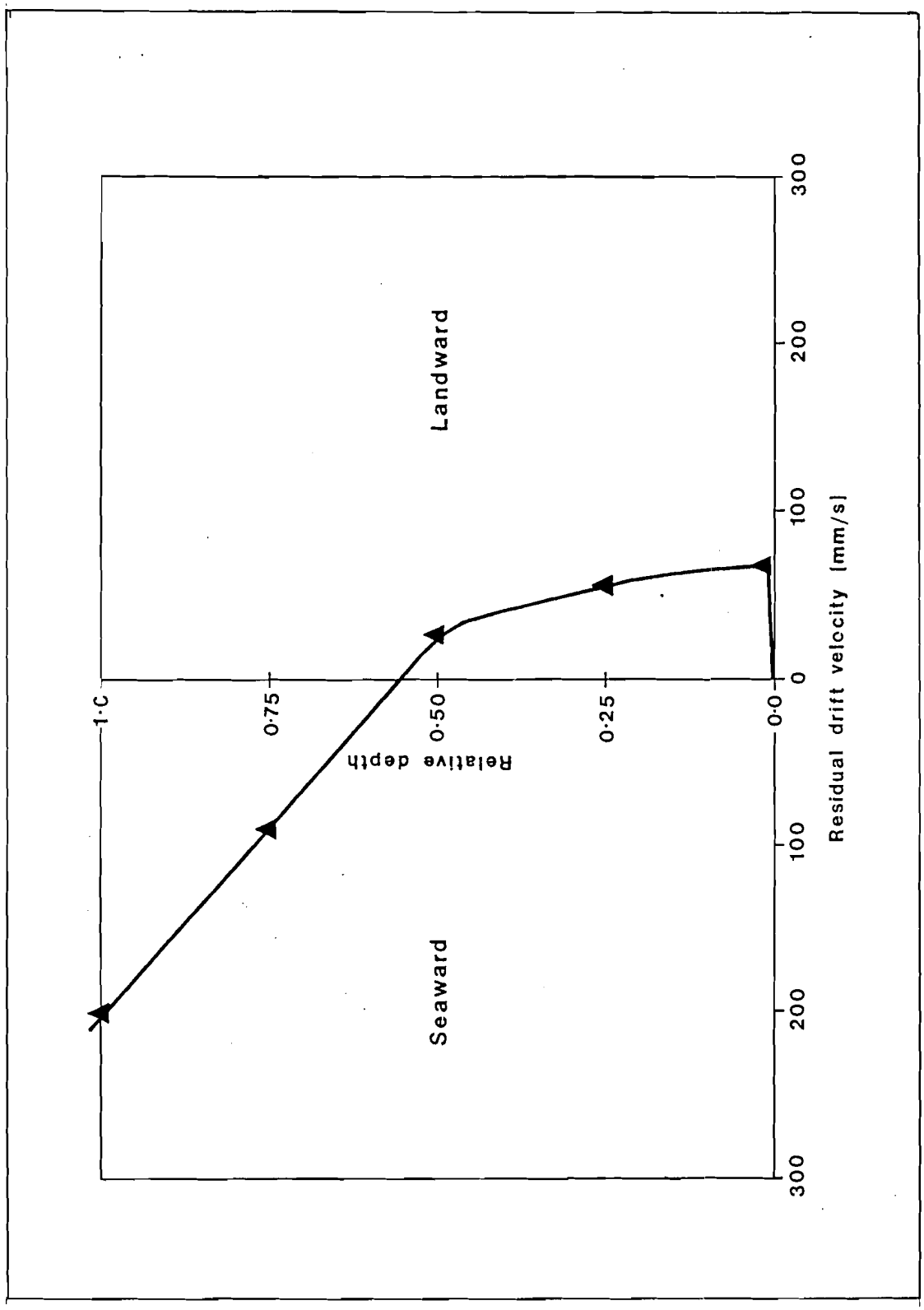

Fig 2 Gravitational circulation in the Mersey Estuary

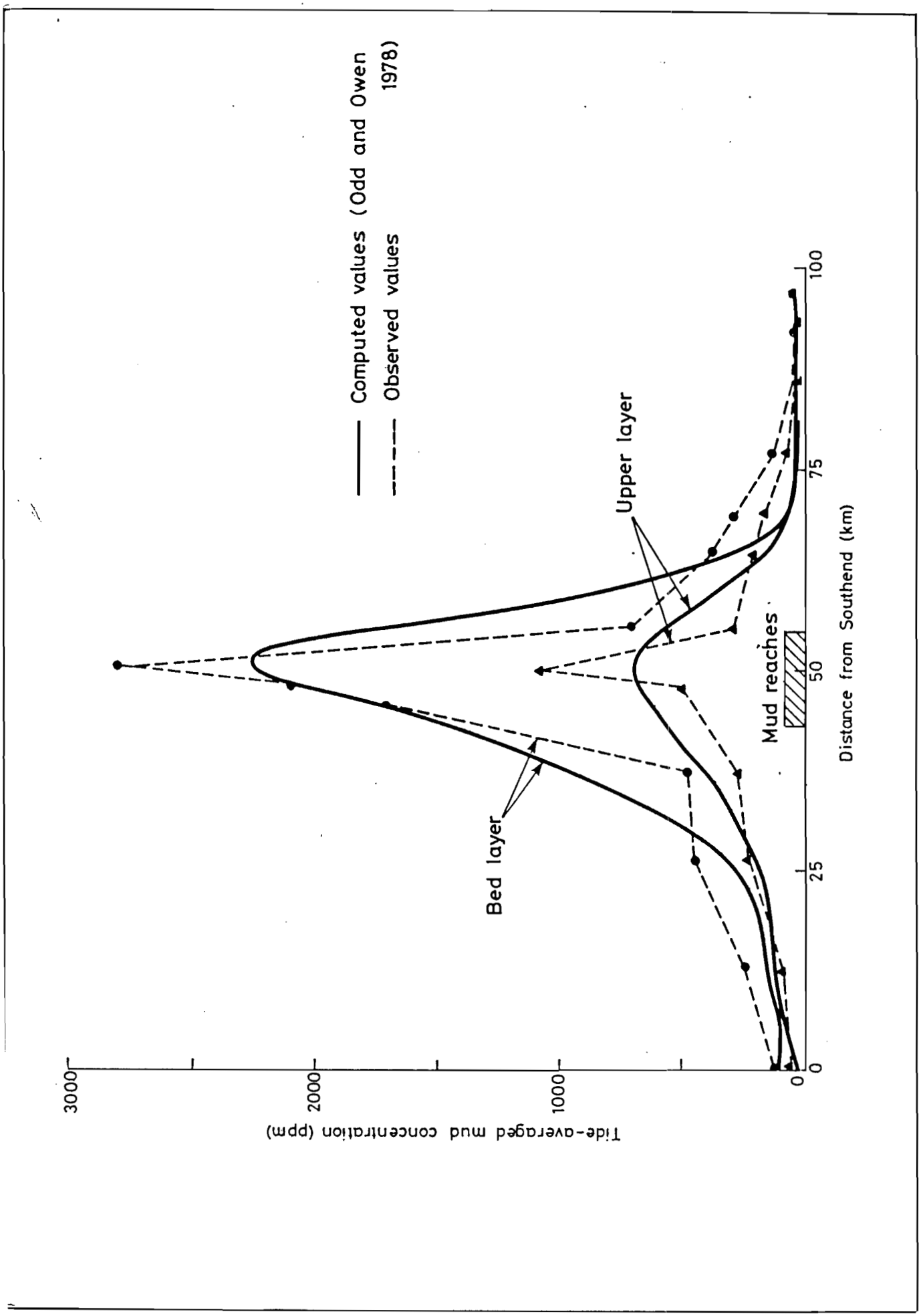

Fig 3 Distribution of suspended mud in the Thames Estuary

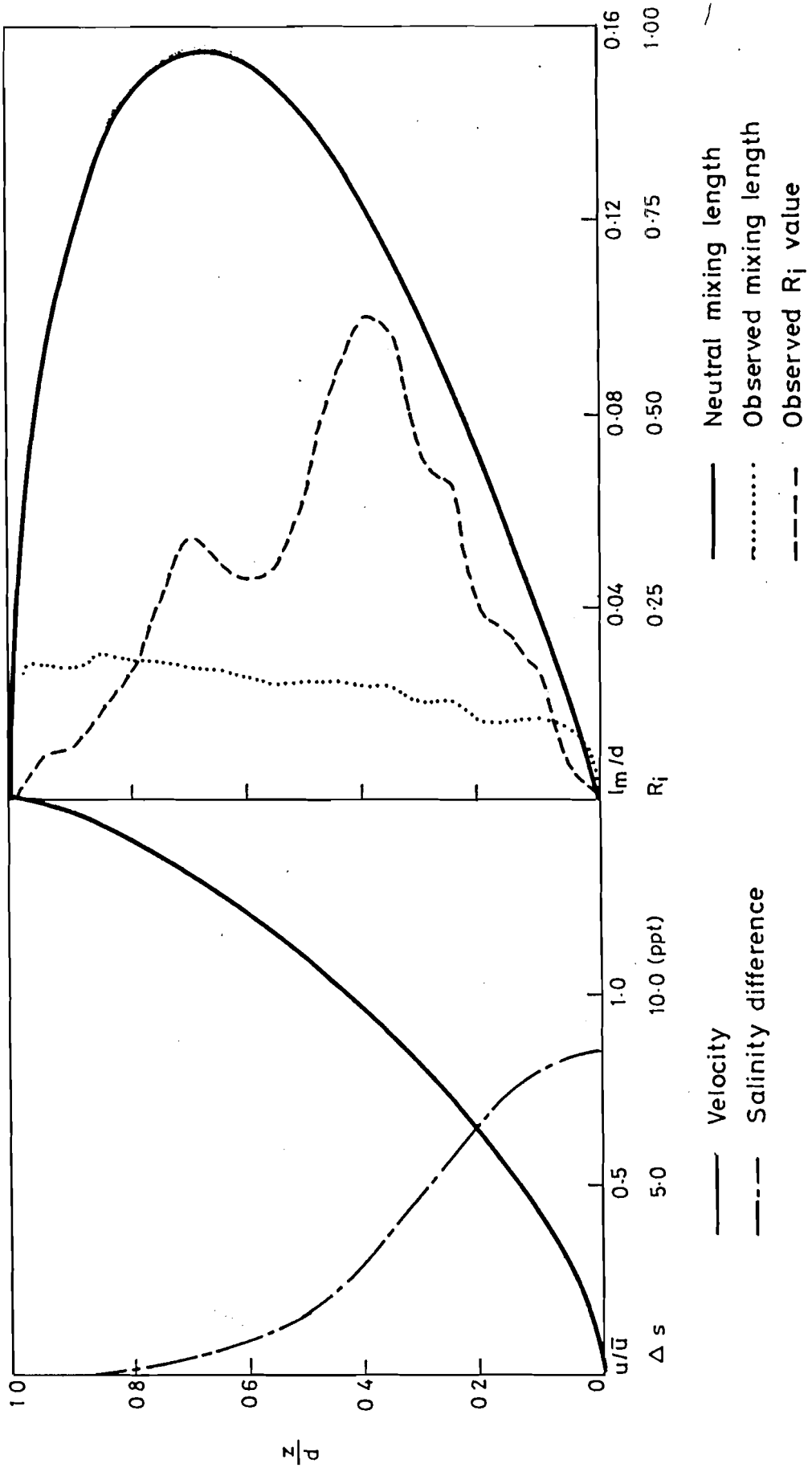

Fig 4 Typical velocity, salinity, R_i and mixing length profiles

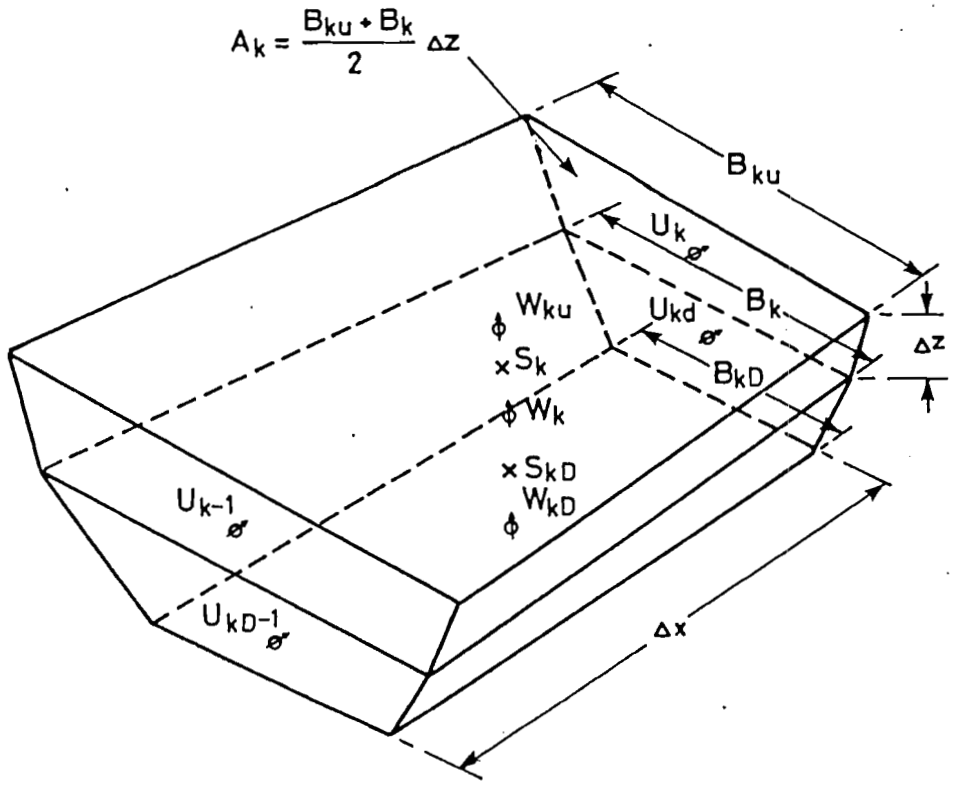

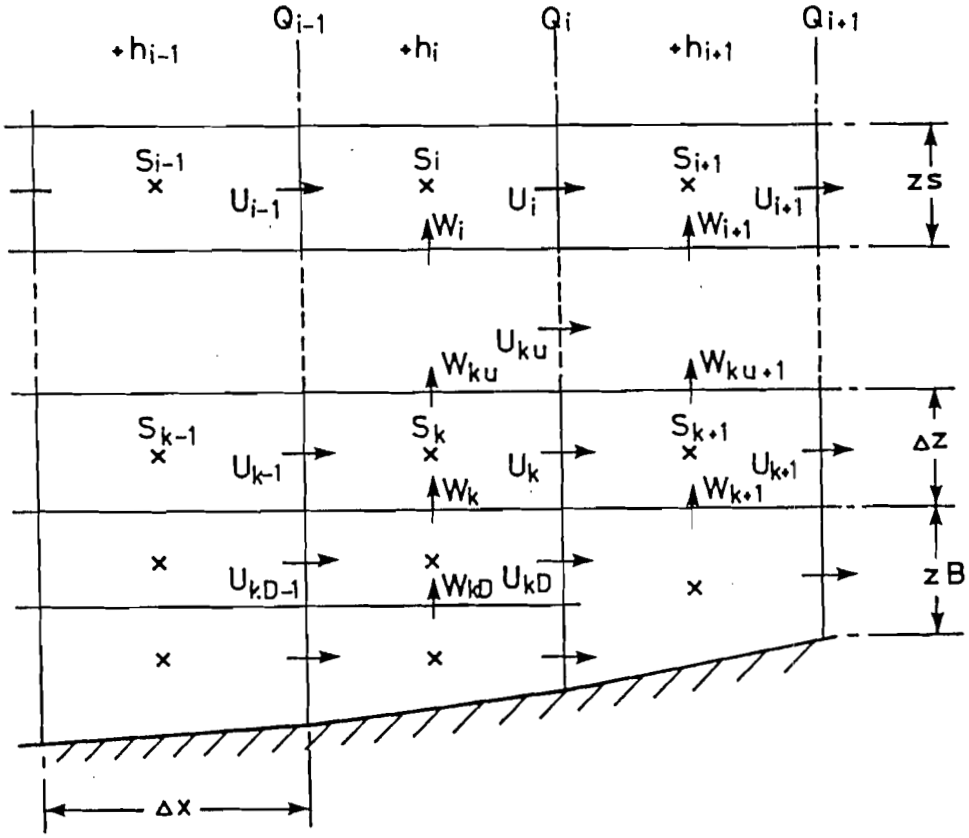

Fig 5 Two-dimensional finite difference grid

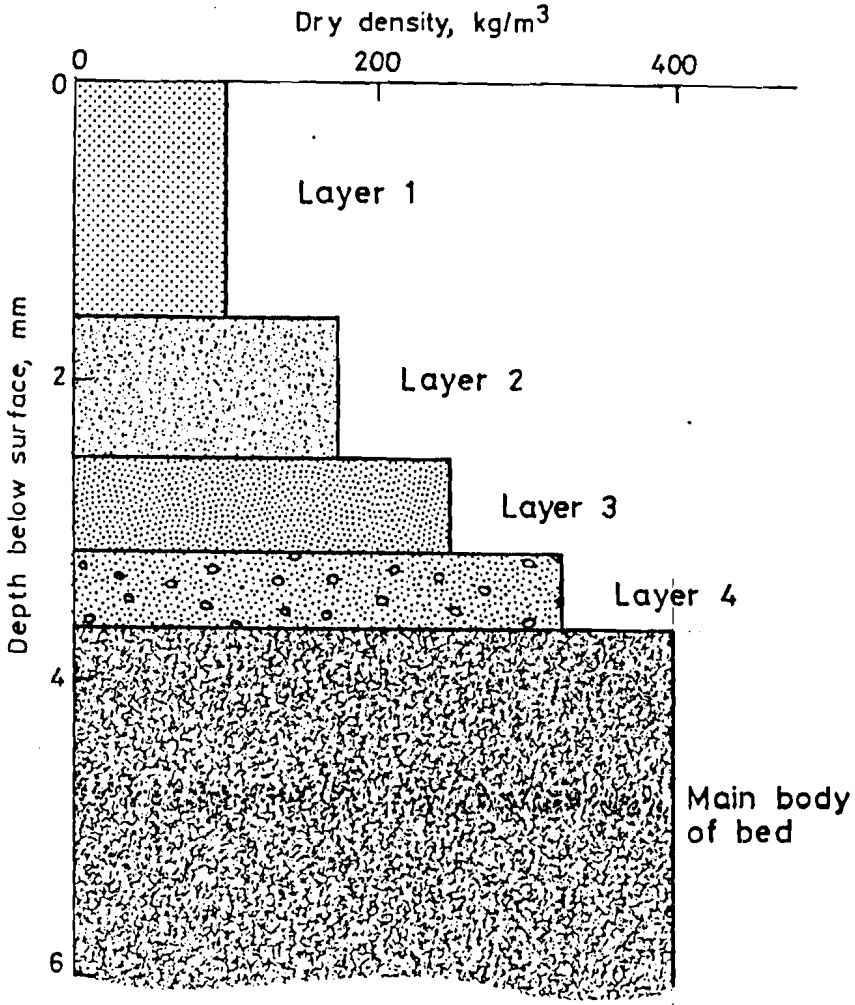

Fig 6 Schematic representation of slack water mud deposits

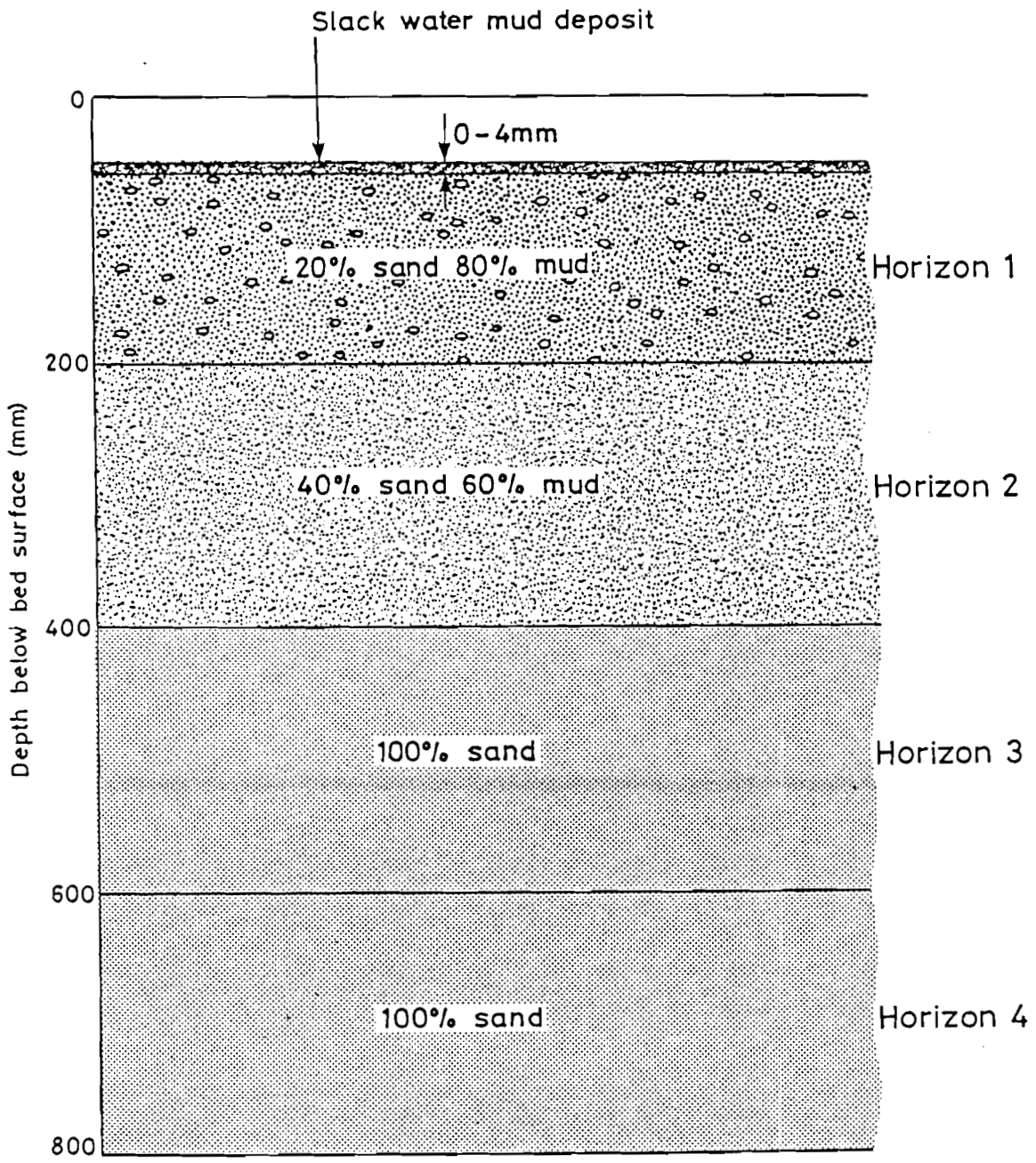

ig 7 Schematic representation of sub-surface mixed sand and mud deposits

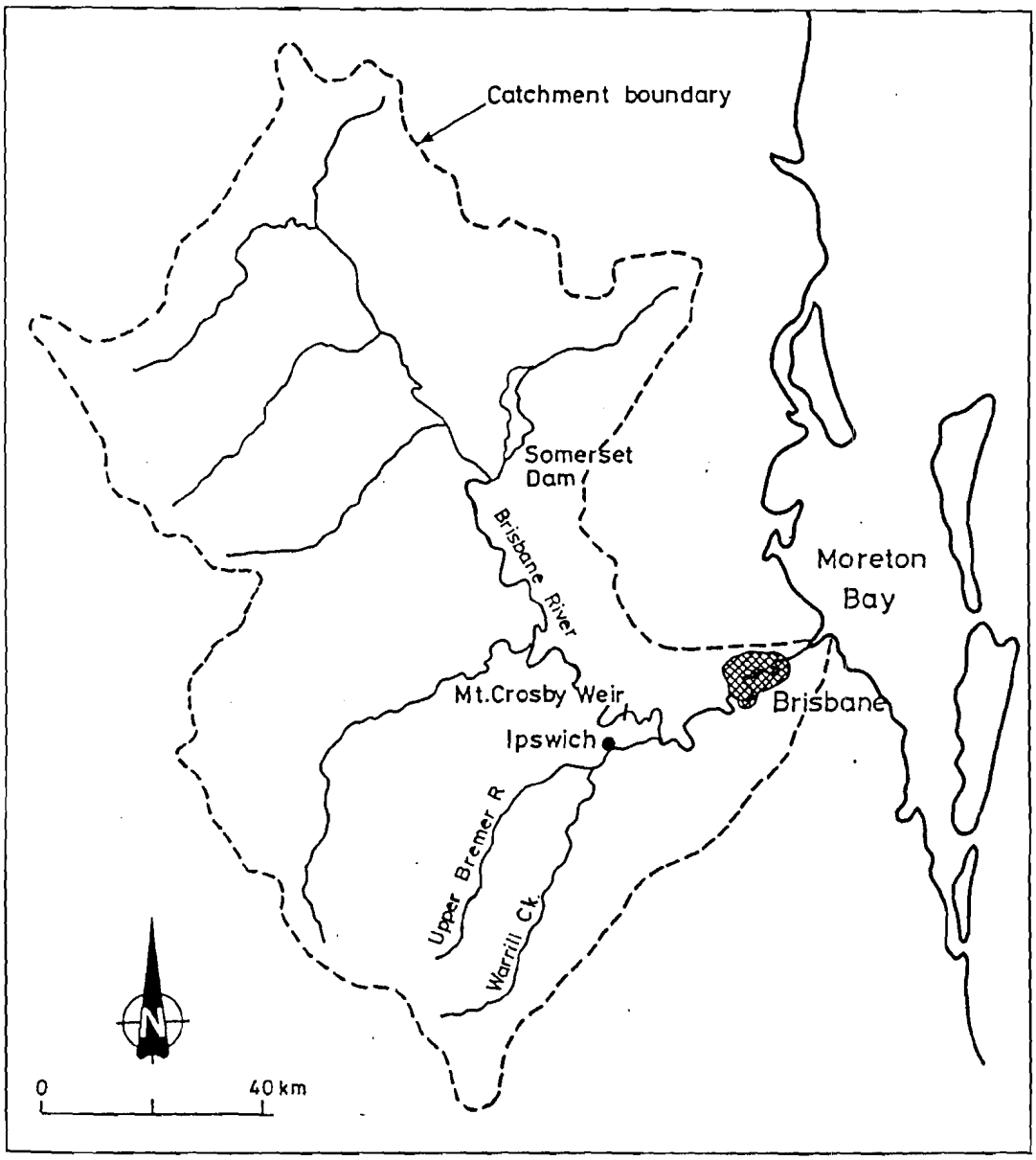

Fig 8 Brisbane River : Location plan

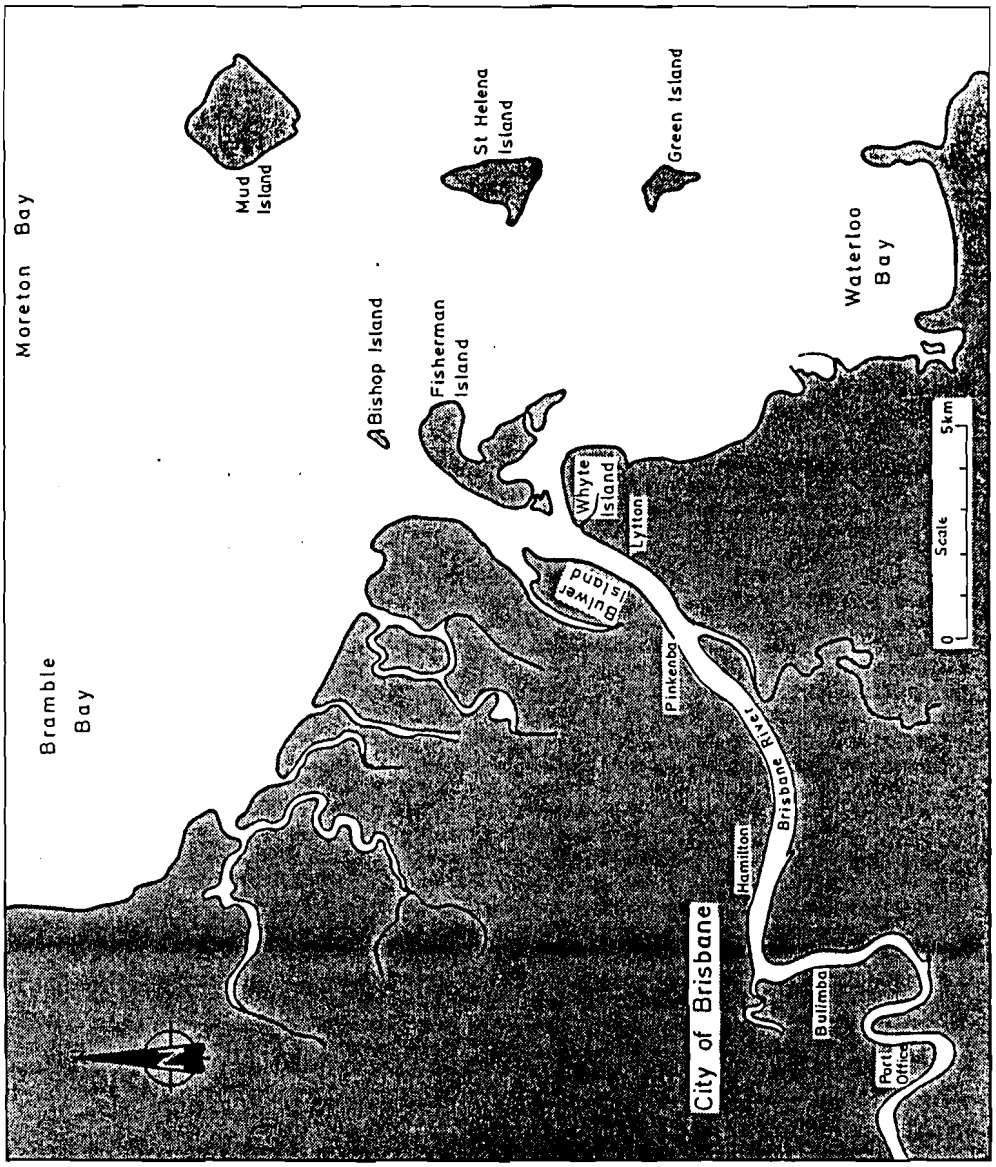

Fig 9 Port of Brisbane. Location plan.

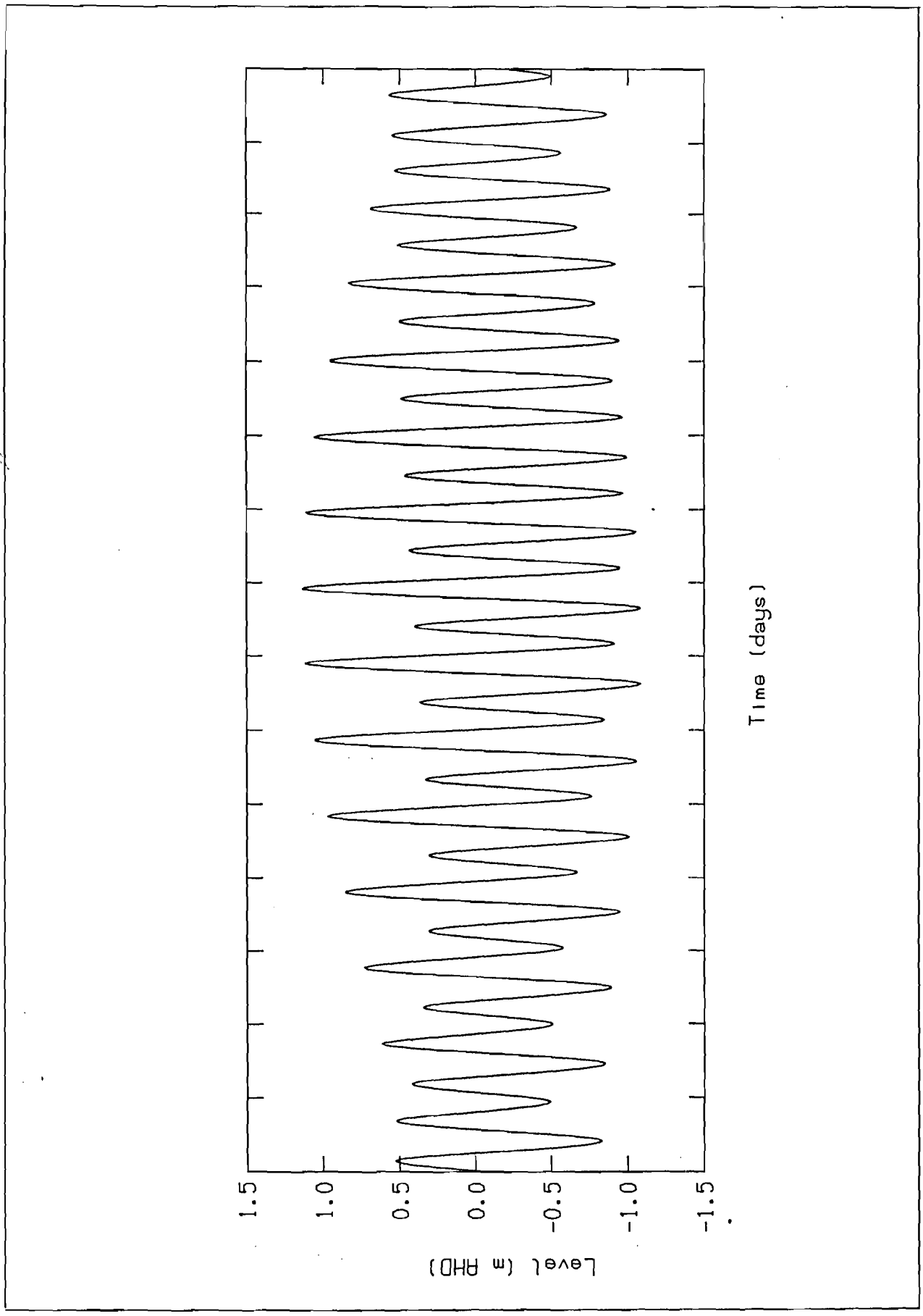

Fig 10 Synthesised neap-spring tidal cycle at West Inner Bar

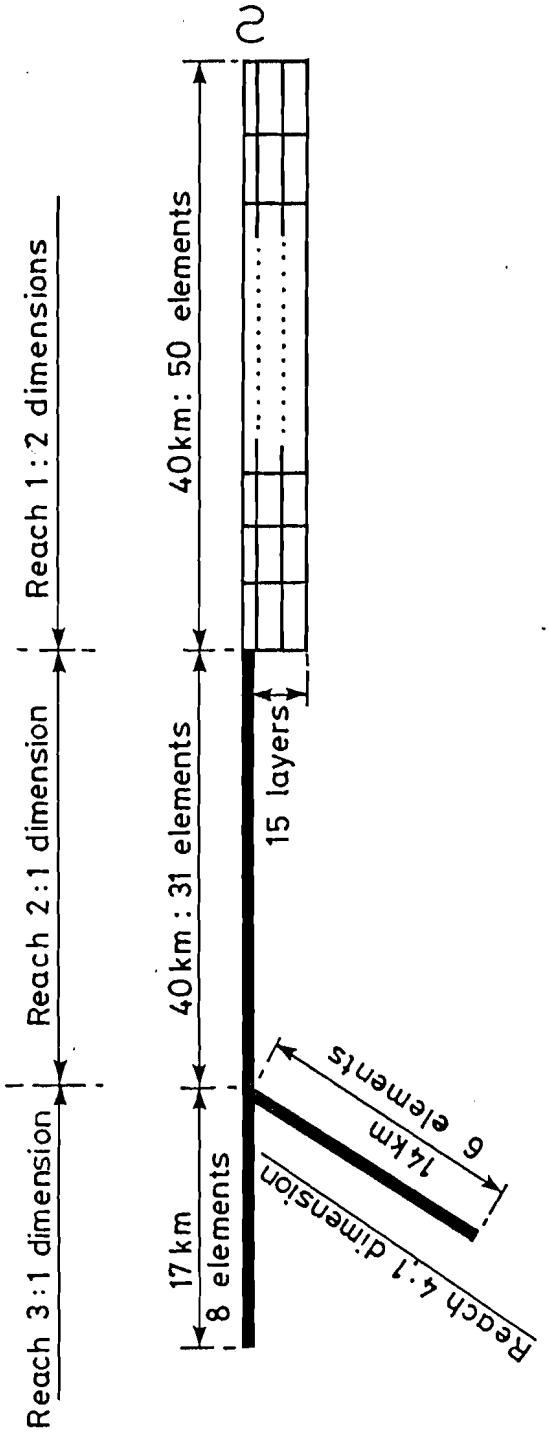

Fig 11 Schematised representation of the Brisbane Estuary

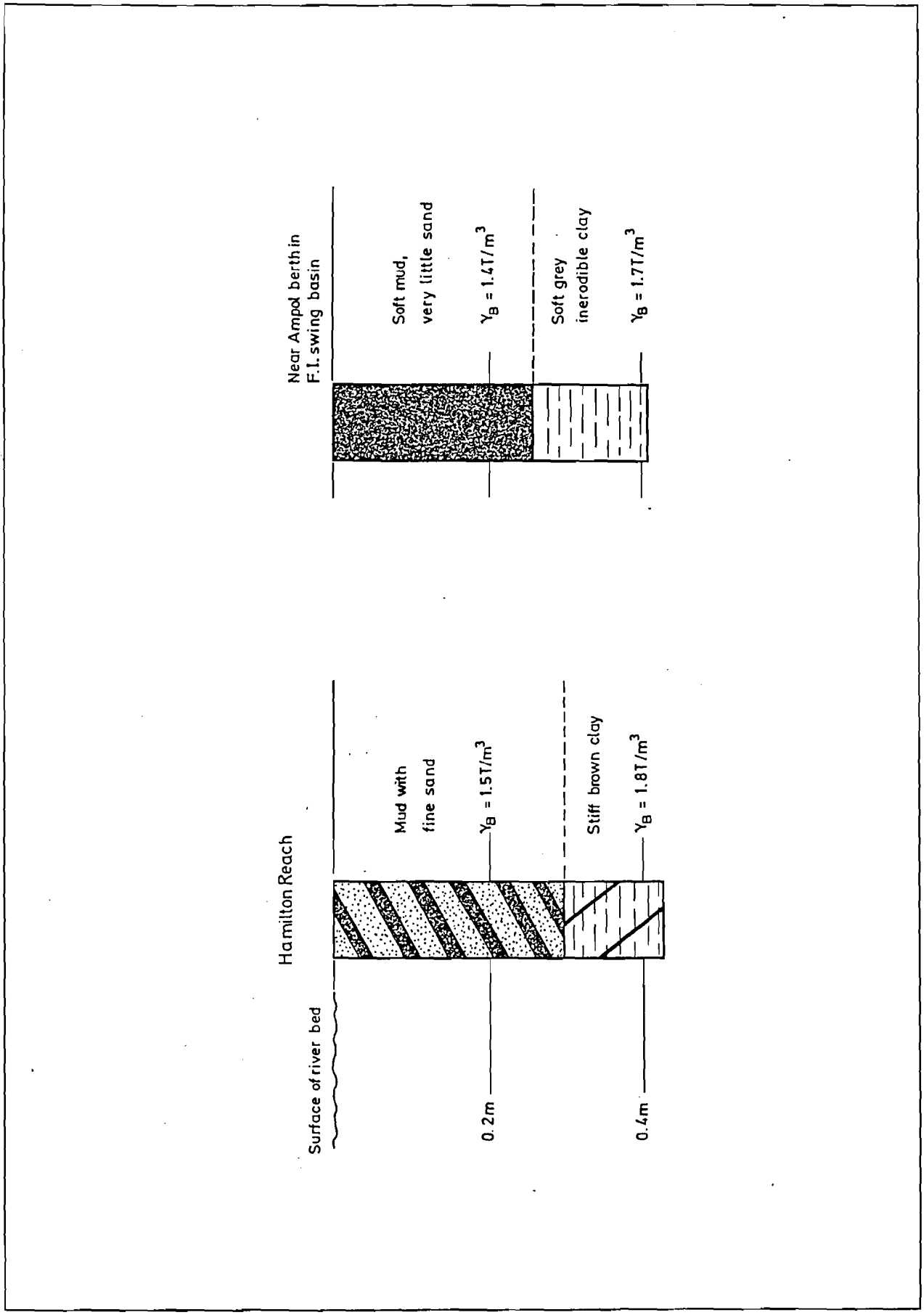

Fig 12 Undisturbed vibro bed cores

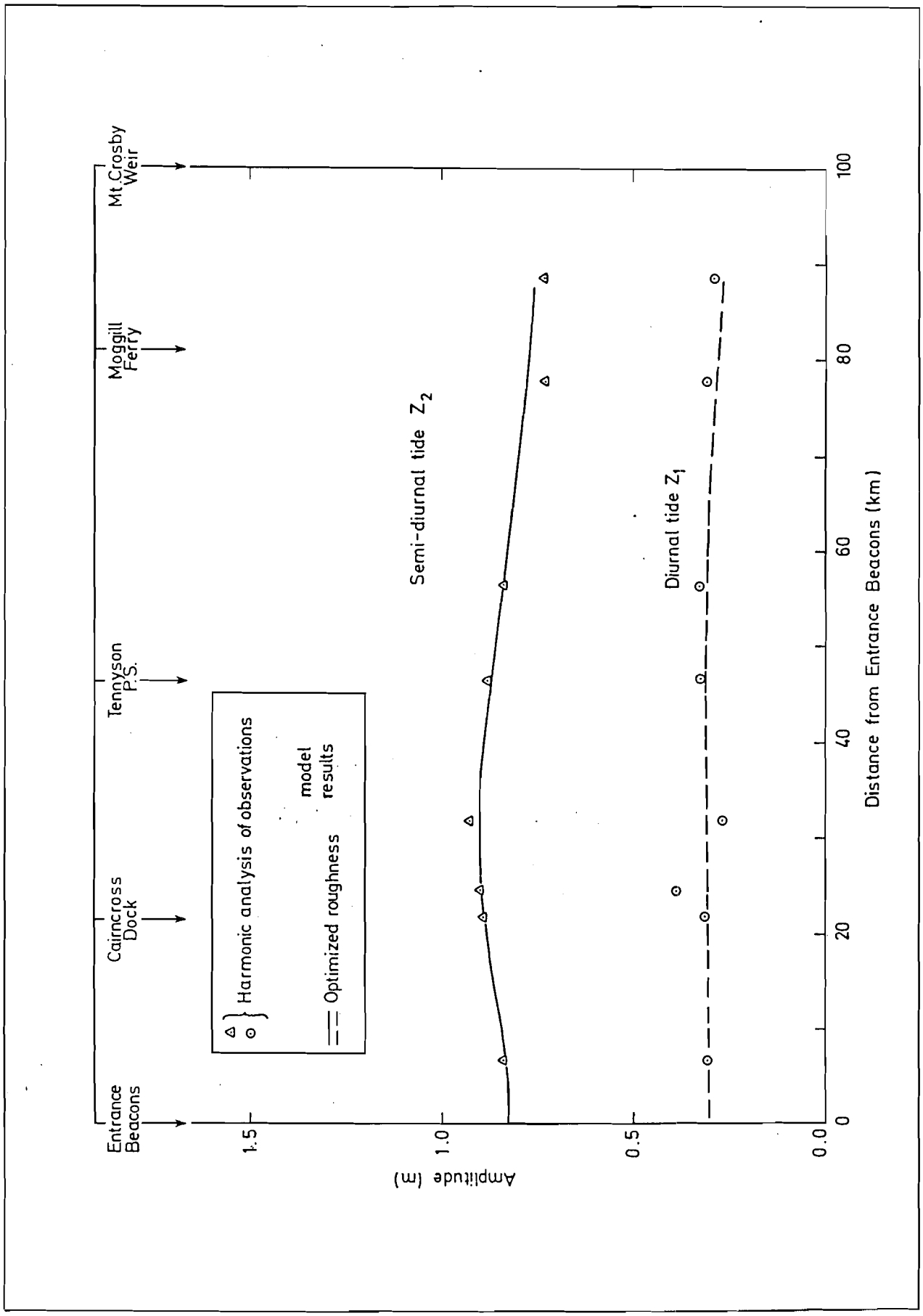

Fig 13 Comparison of simulated and observed tidal amplitudes

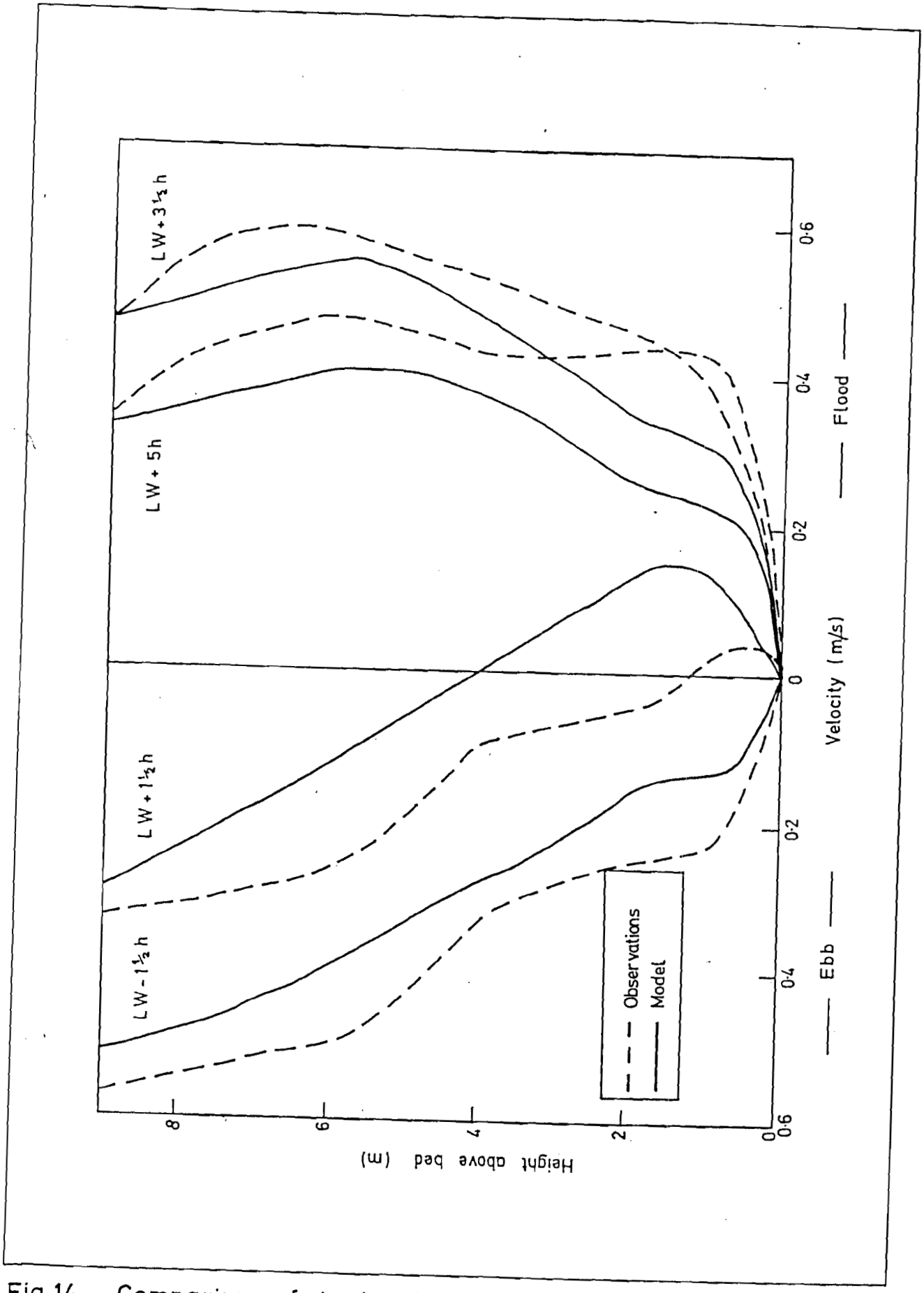

Fig 14 Comparison of simulated and observed velocity profiles in the port area – dry season

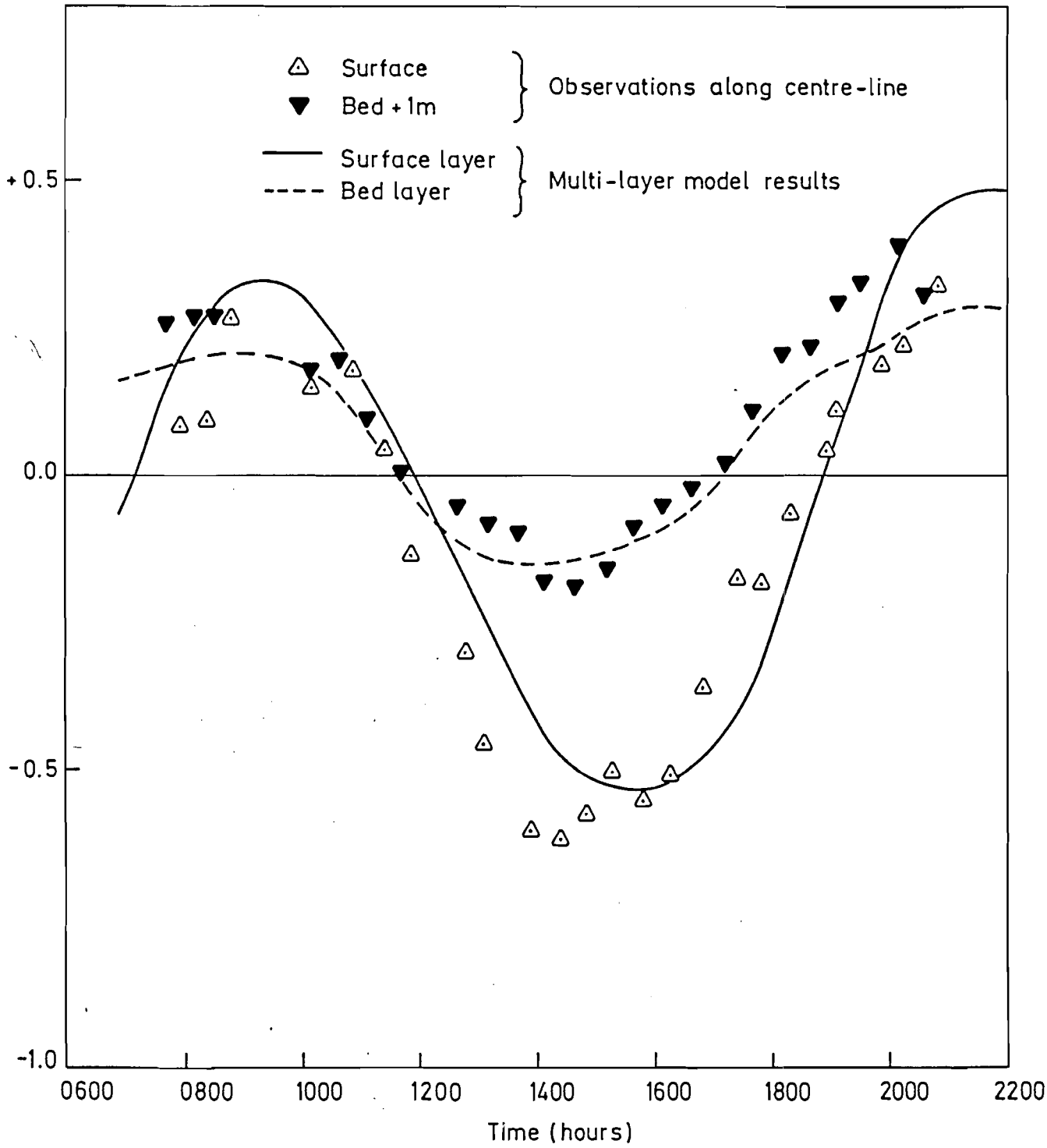

ig 15 Comparison of simulated and observed velocities at bed and surface in port area - dry season

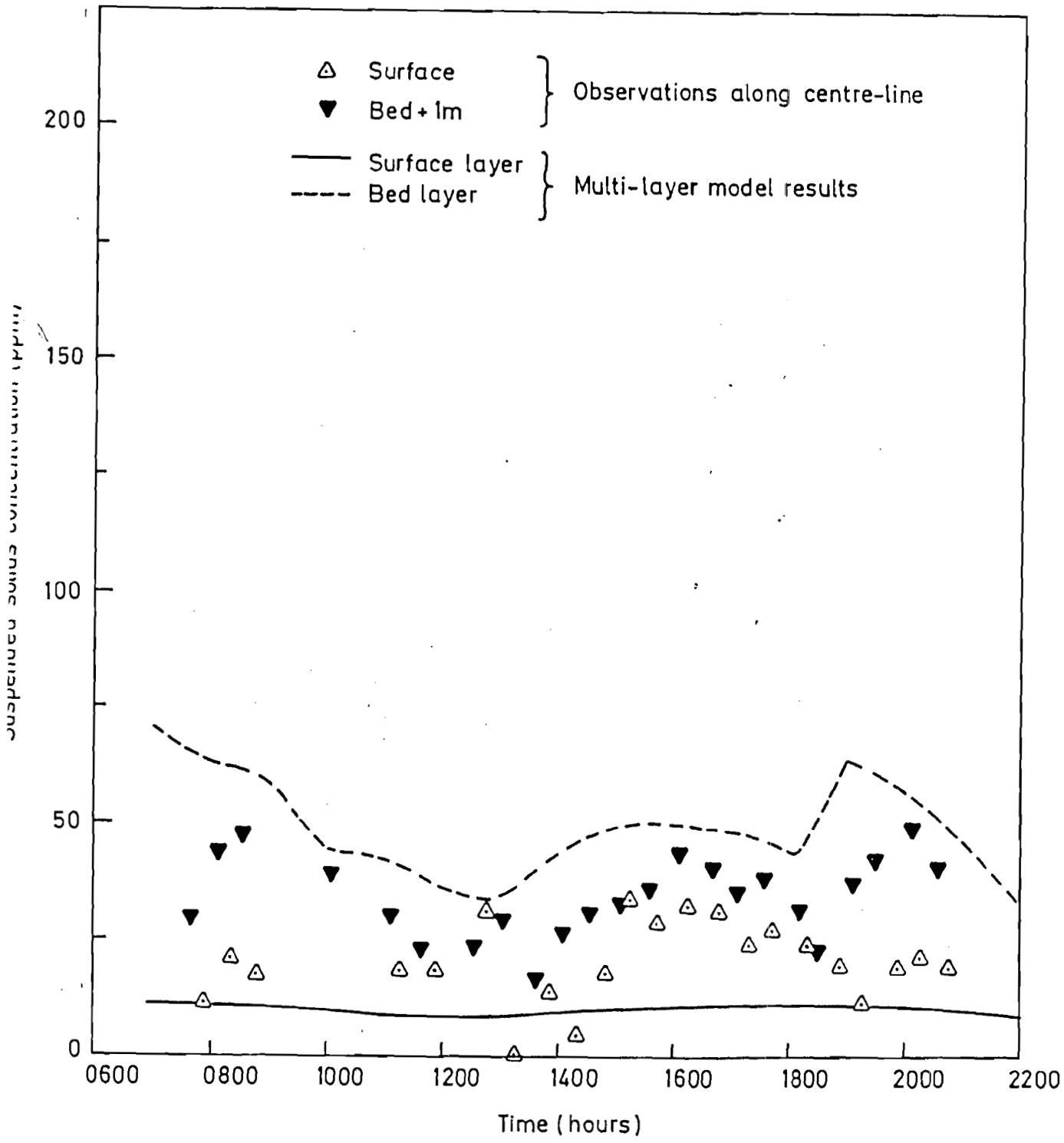

Fig 16 Comparison of simulated and observed mud concentrations in the port area - dry season

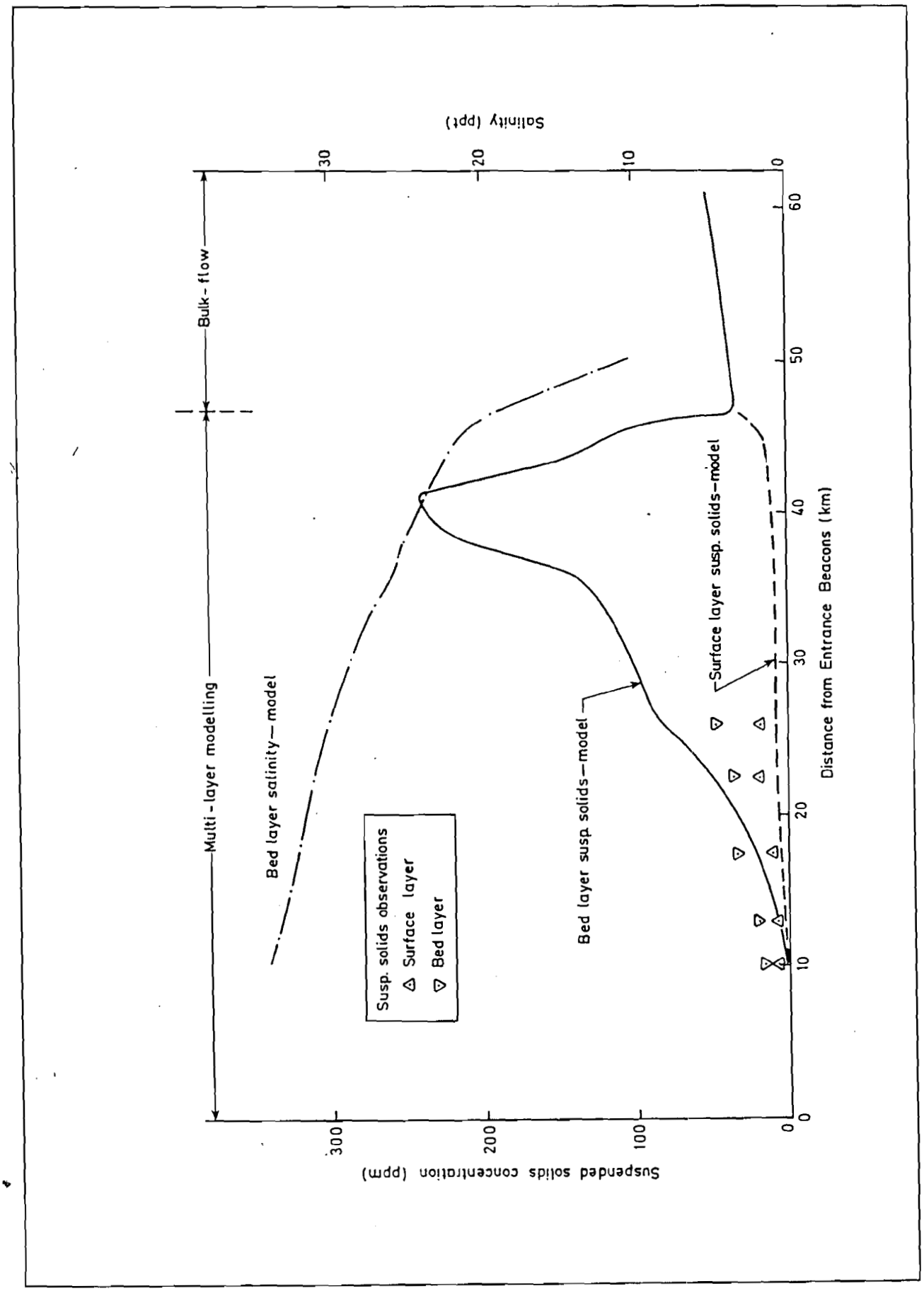

Fig 17 Tide-averaged suspended solids and salinity- model and observations - dry season

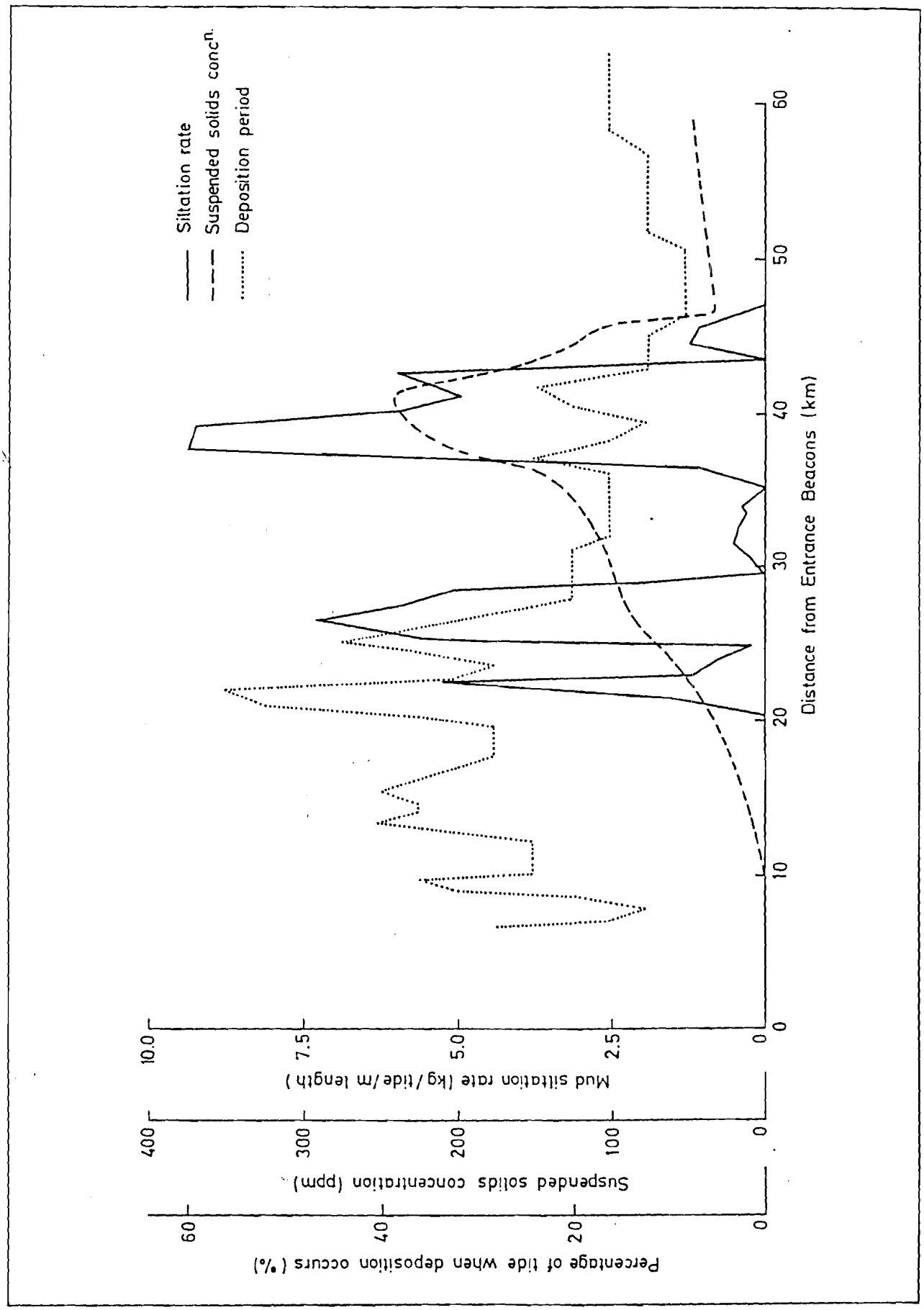

Fig 18 Hindcast mud siltation pattern - 1977 dry season

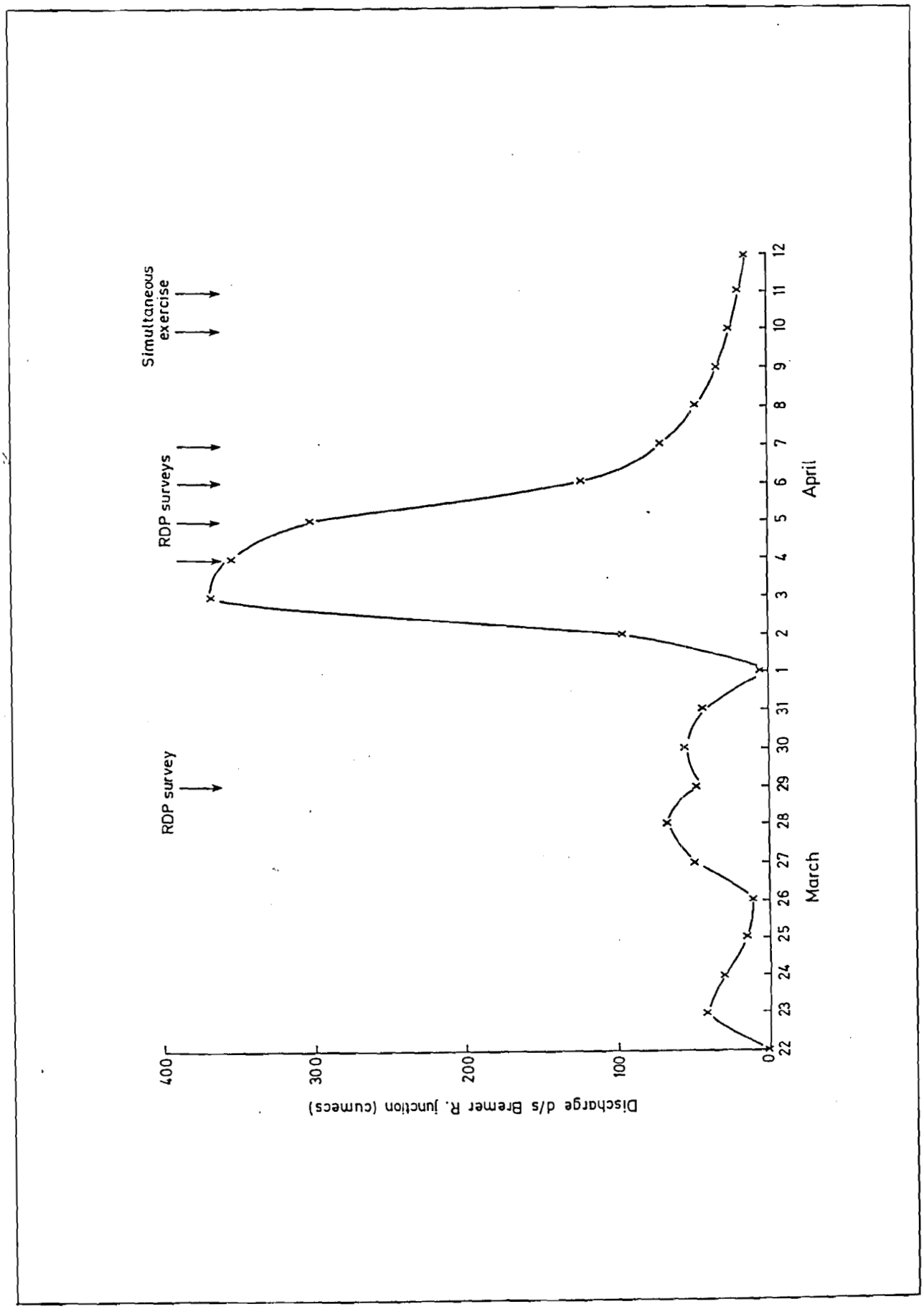

Fig 19 First fluvial flood hydrograph-1978 wet season

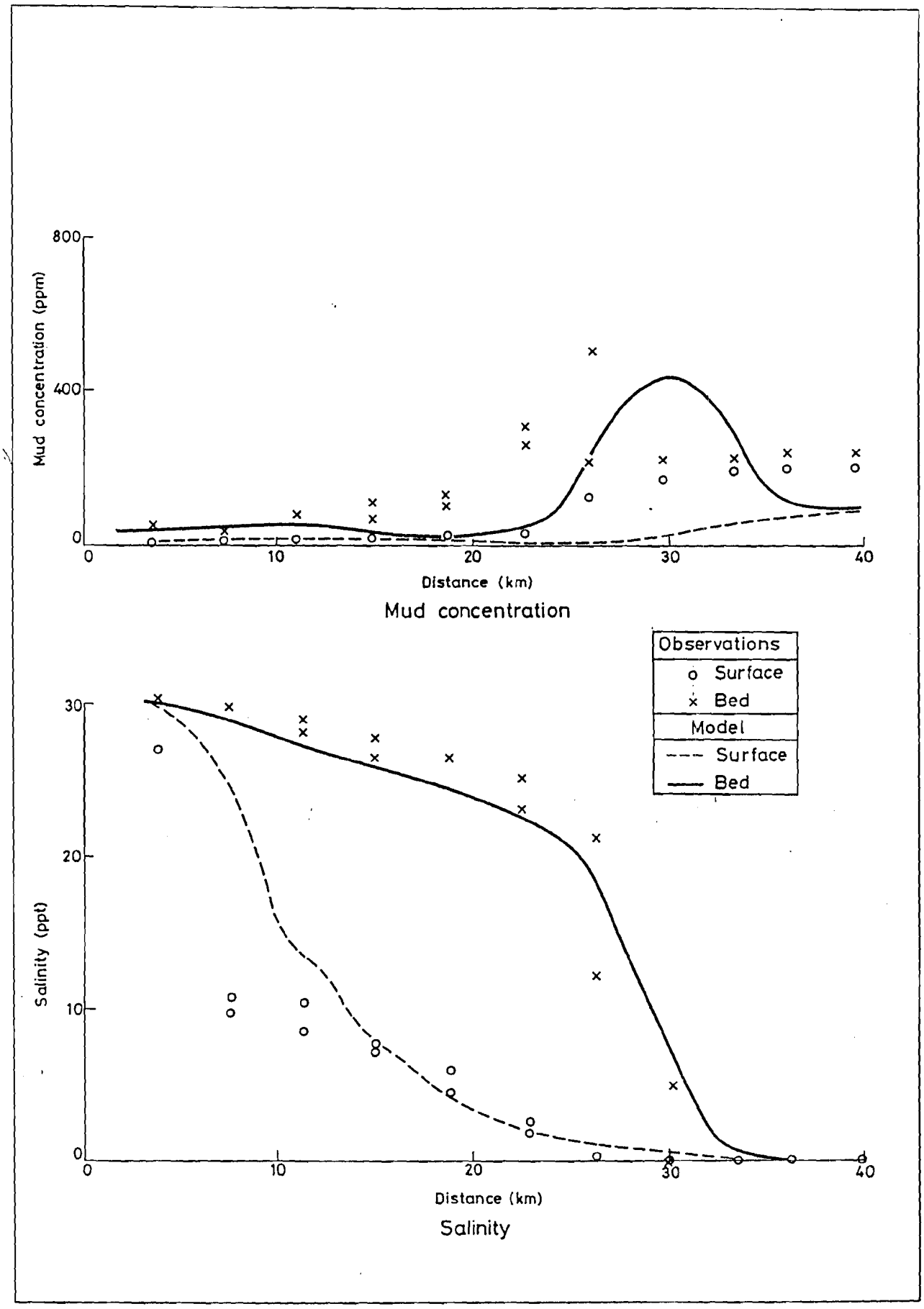

Fig 20 1600 hours 4th April 1978

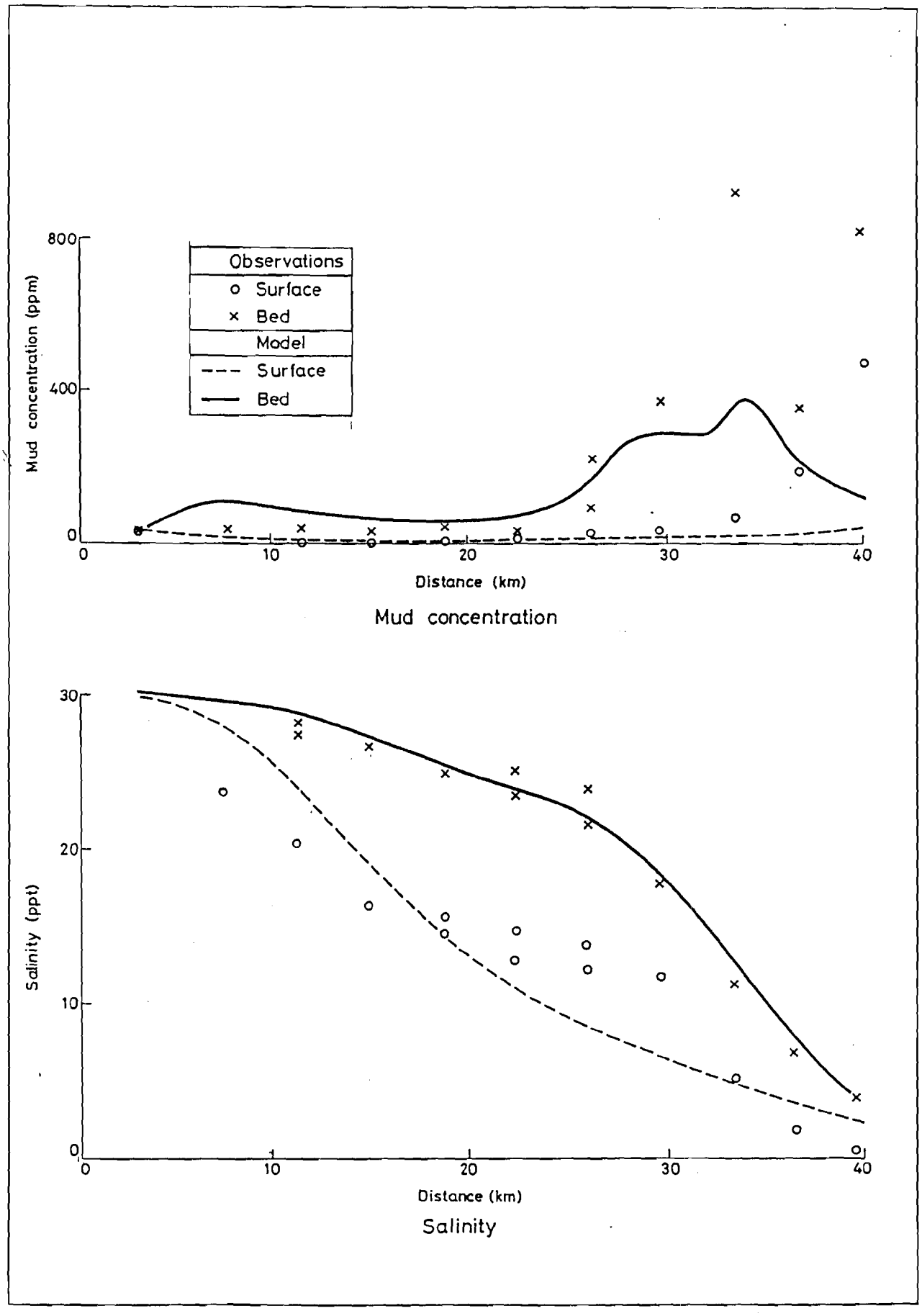

Fig 21 1300 hours 7th April 1978

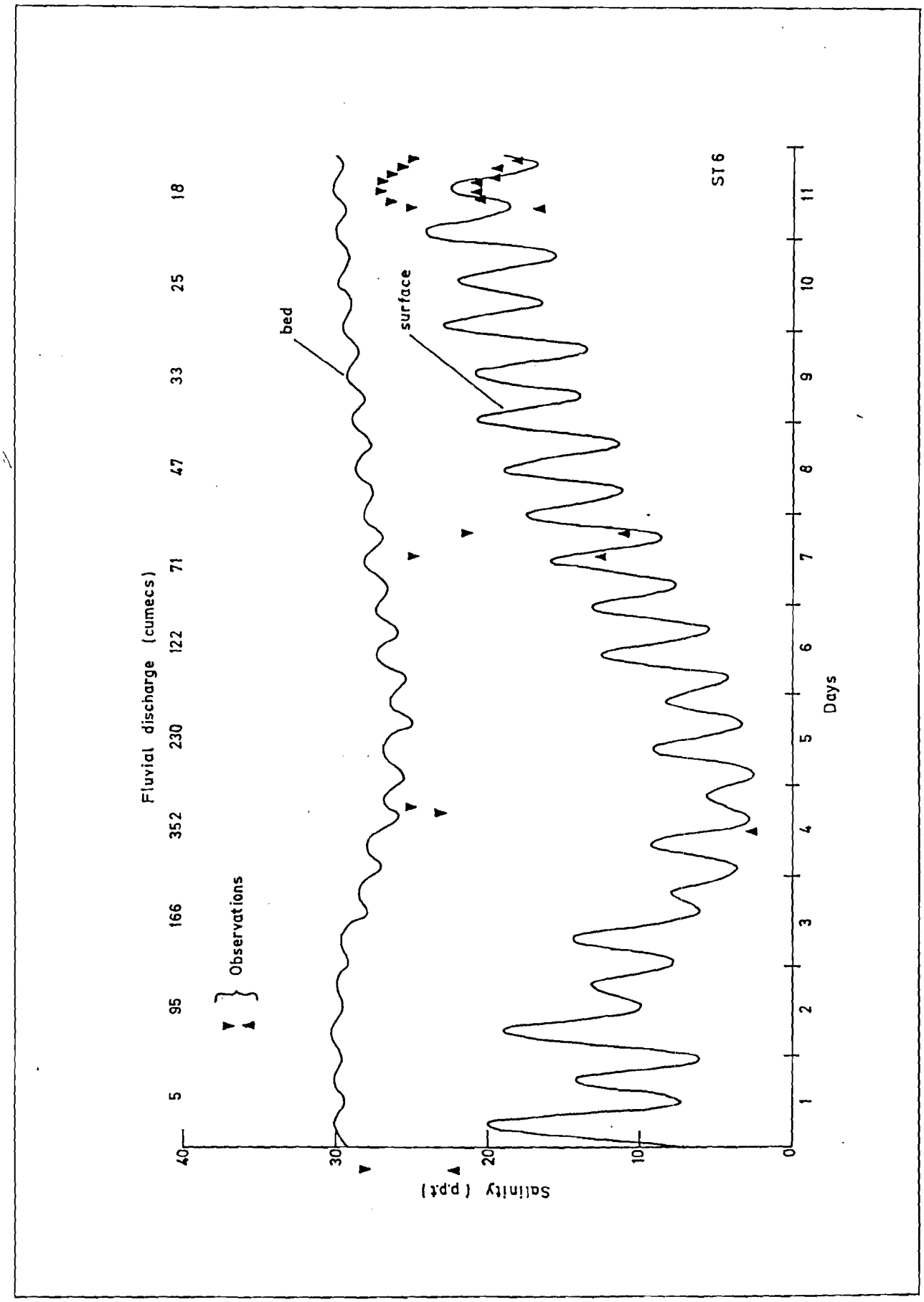

Fig 22 Comparison of simulated and observed salinities in Hamilton Reach 1-12.4.78

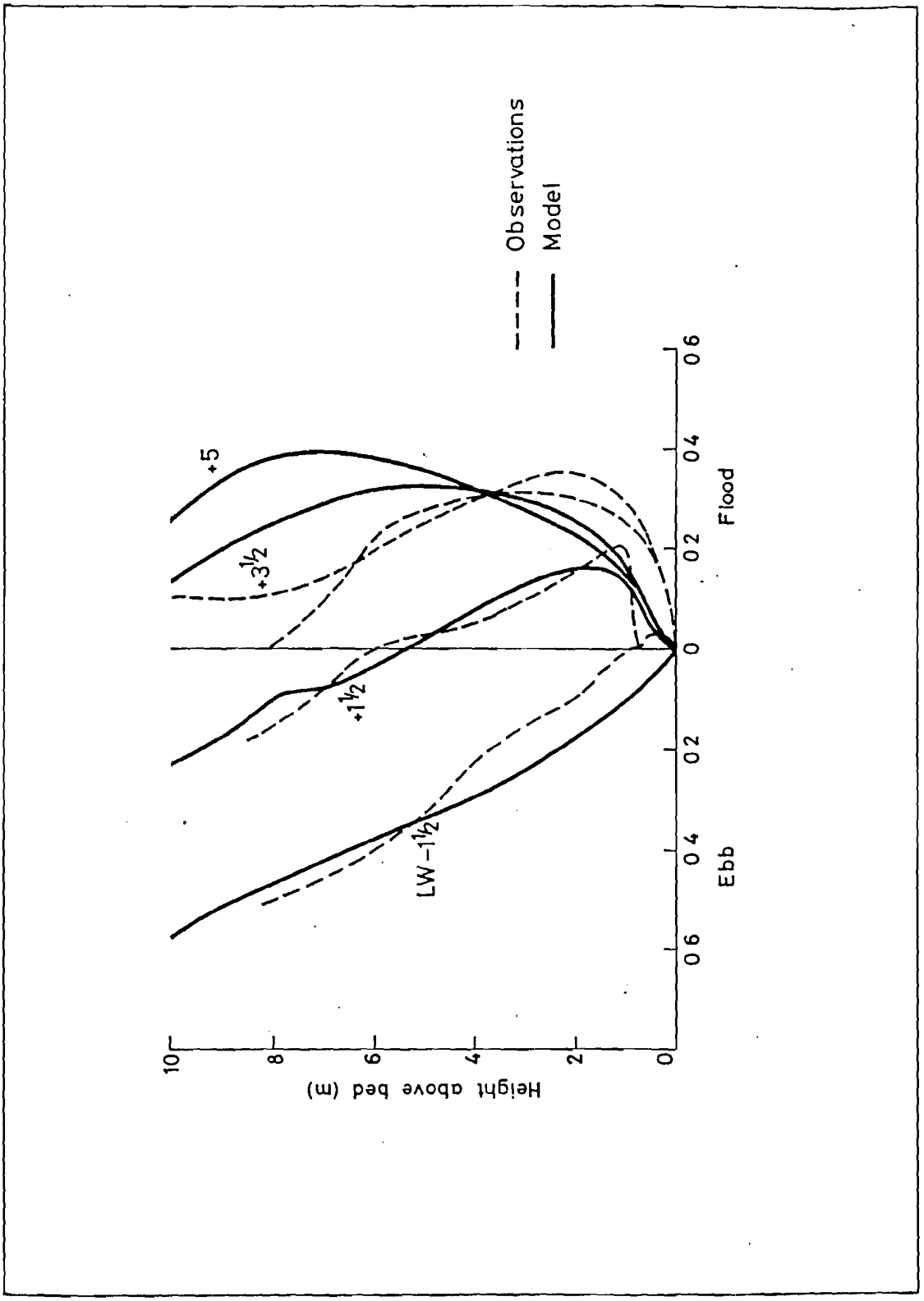

Fig 23 Comparison of simulated and observed velocity profiles 11.4.78.

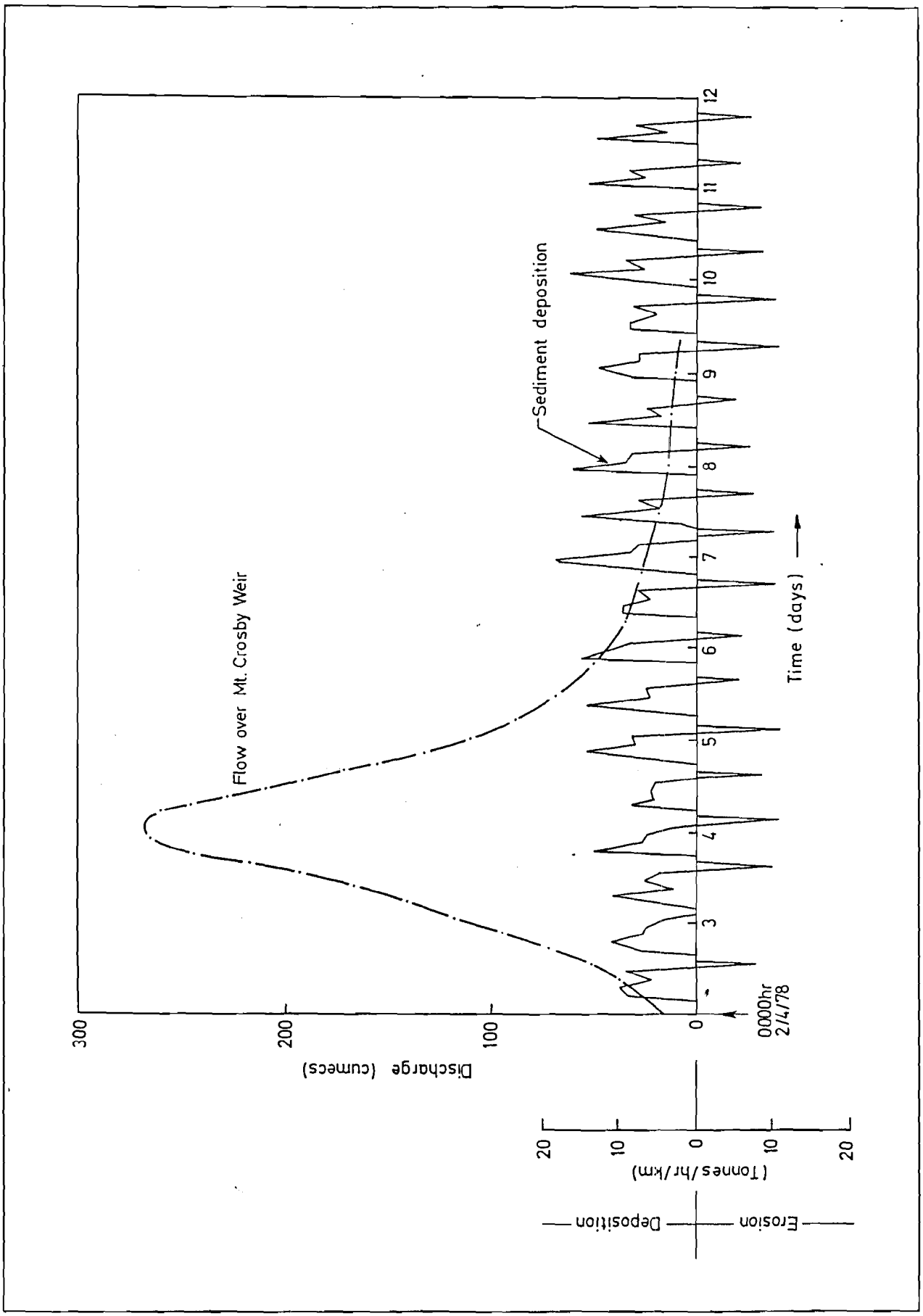

Fig 24 Pattern of deposition and erosion in Hamilton Reach 2-12 April 1978

ɟ 25 Schematic representation of sedimentation processes in the Brisbane River Estuary : wet season

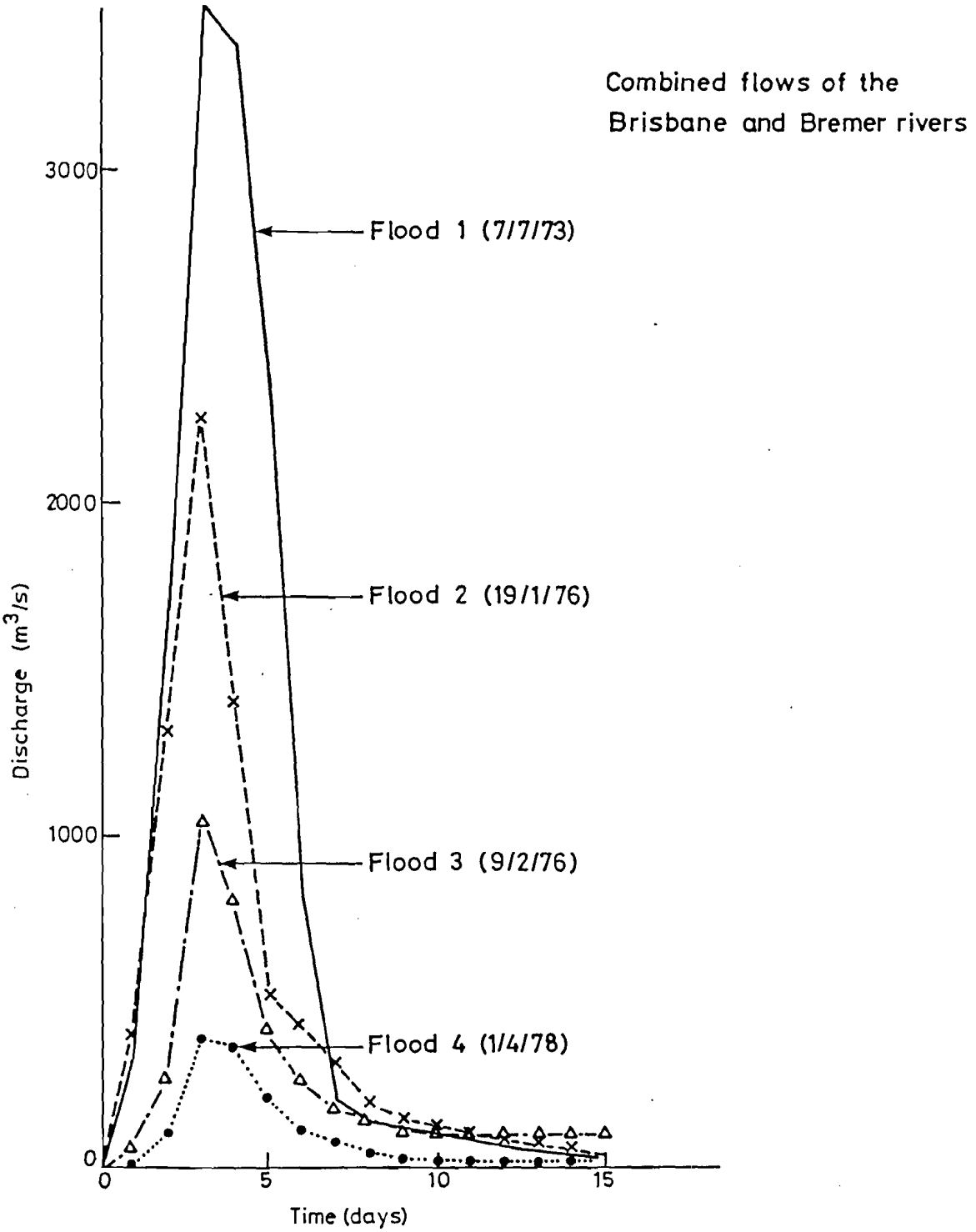

Fig 26 Flood hydrographs

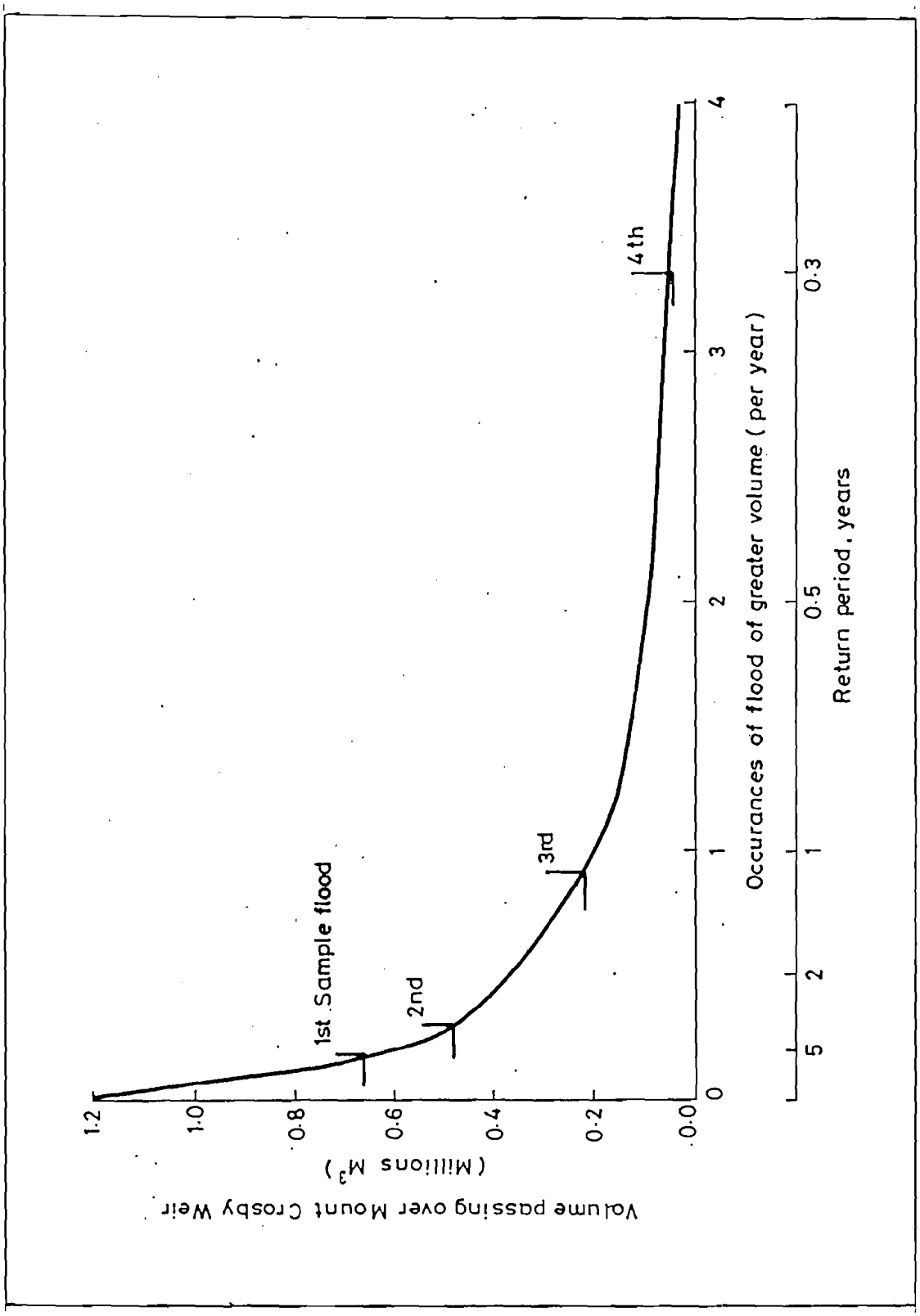

Fig 27 Flood frequency as a function of flood volume

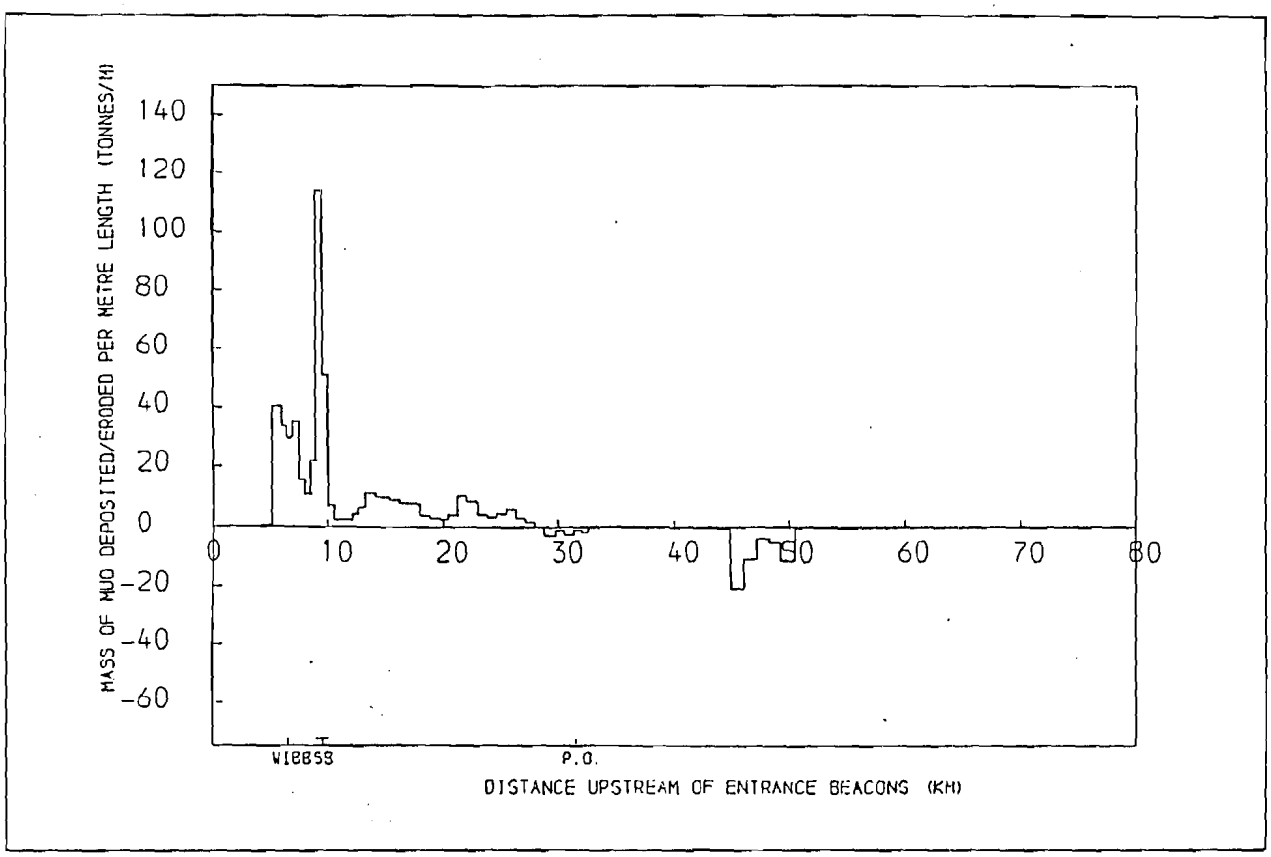

Fig 28 Predicted longitudinal distribution of mud siltation - Flood 1

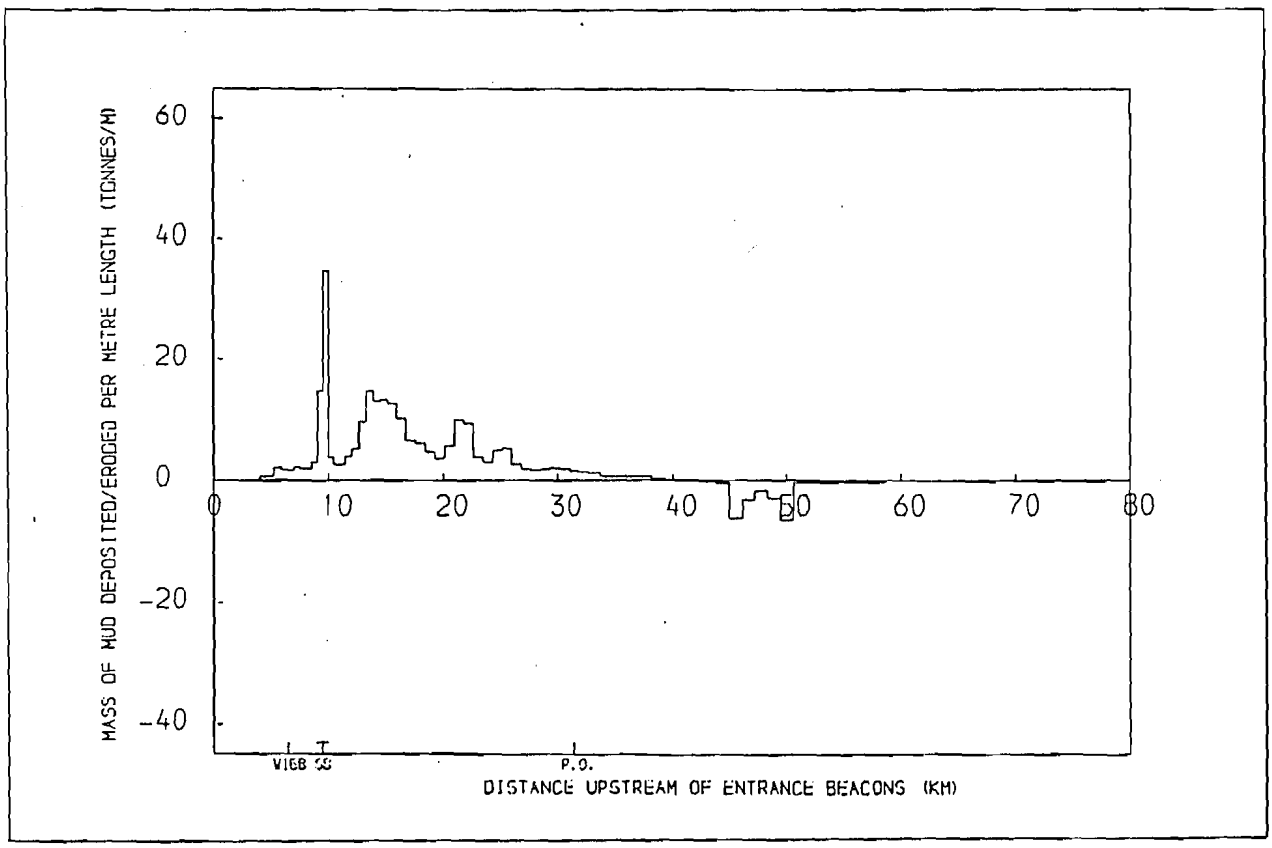

Fig 29 Predicted longitudinal distribution of mud siltation - Flood 2

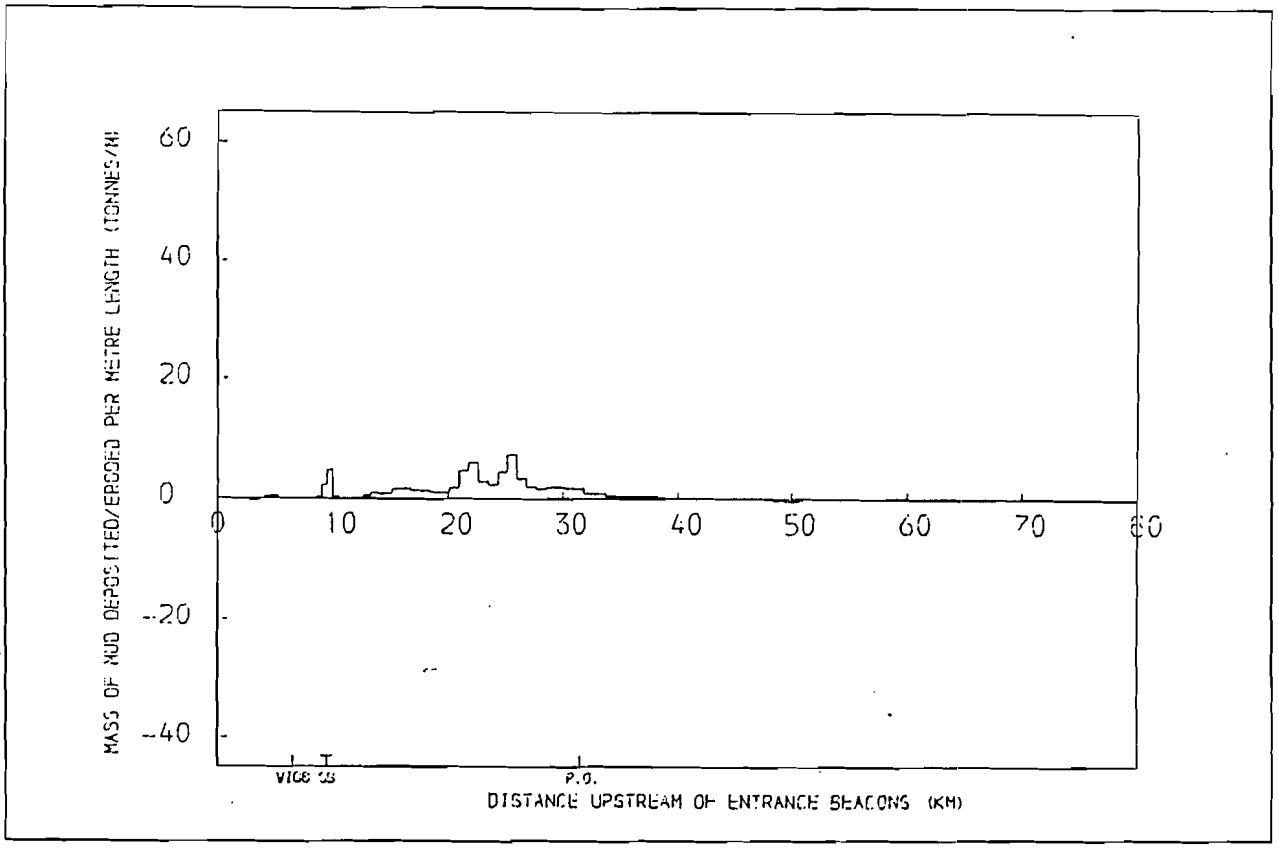

Fig 30 Predicted longitudinal distribution of mud siltation - Flood 3

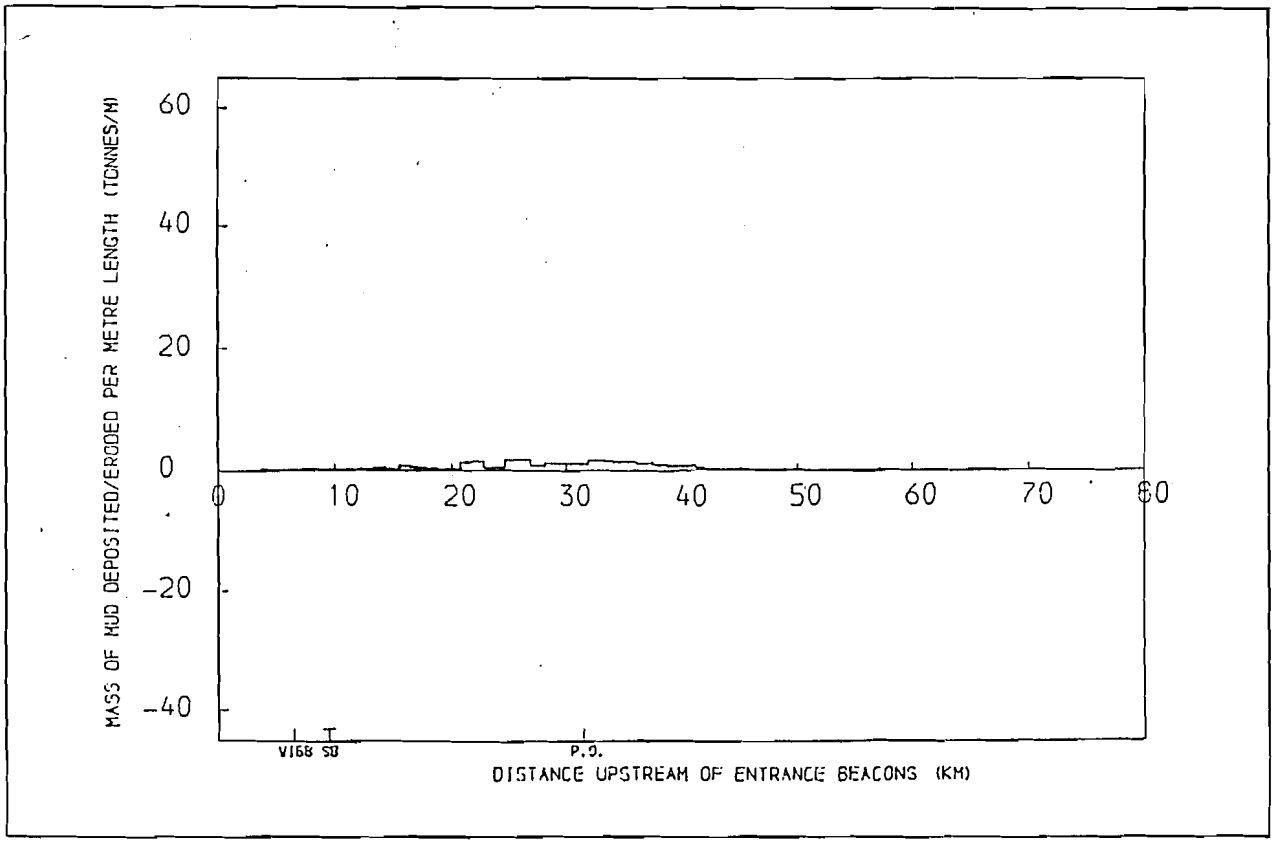

Fig 31 Predicted longitudinal distribution of mud siltation - Flood 4

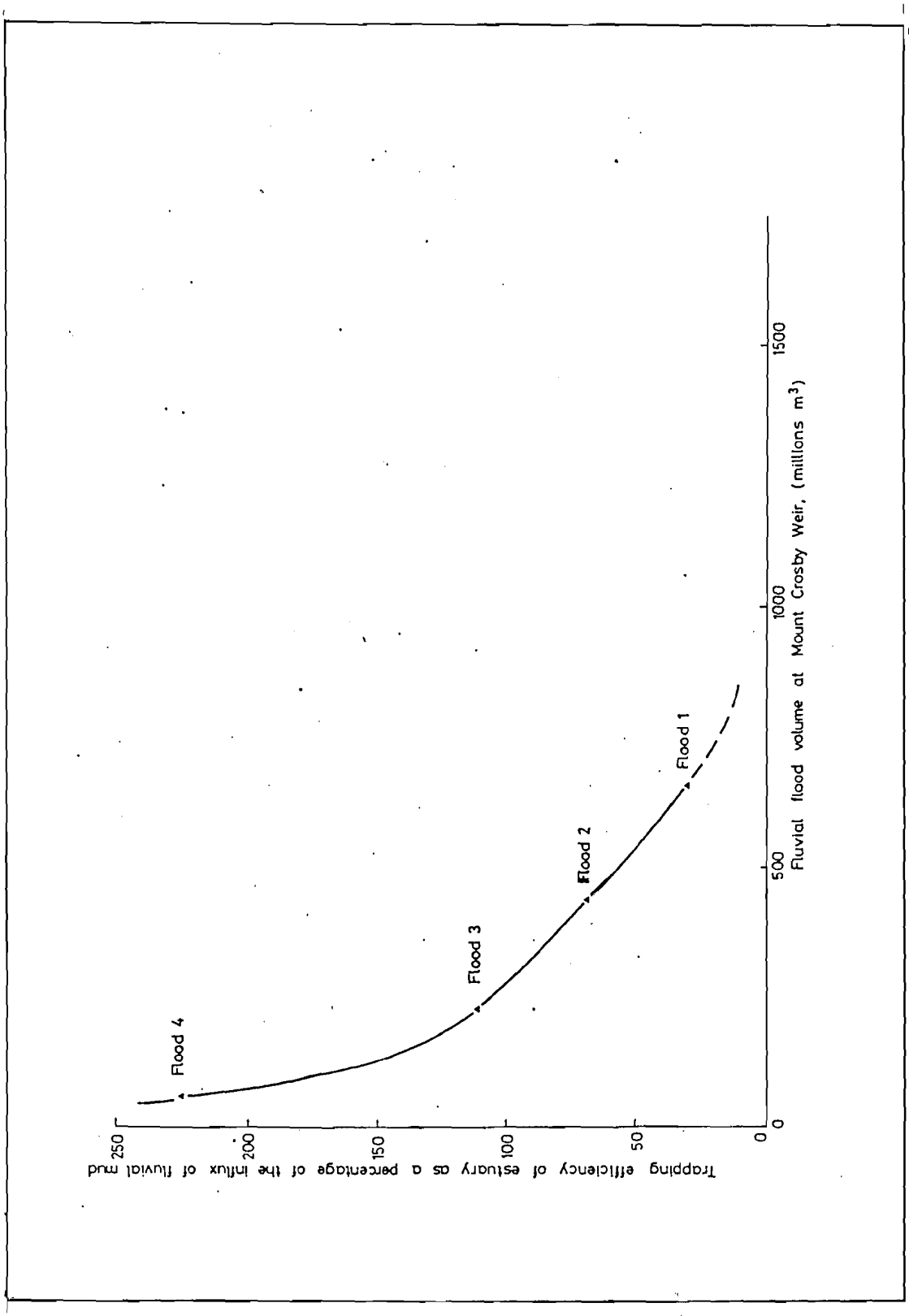

Fig 32 Trapping efficiency of estuary as function of fluvial flood volume

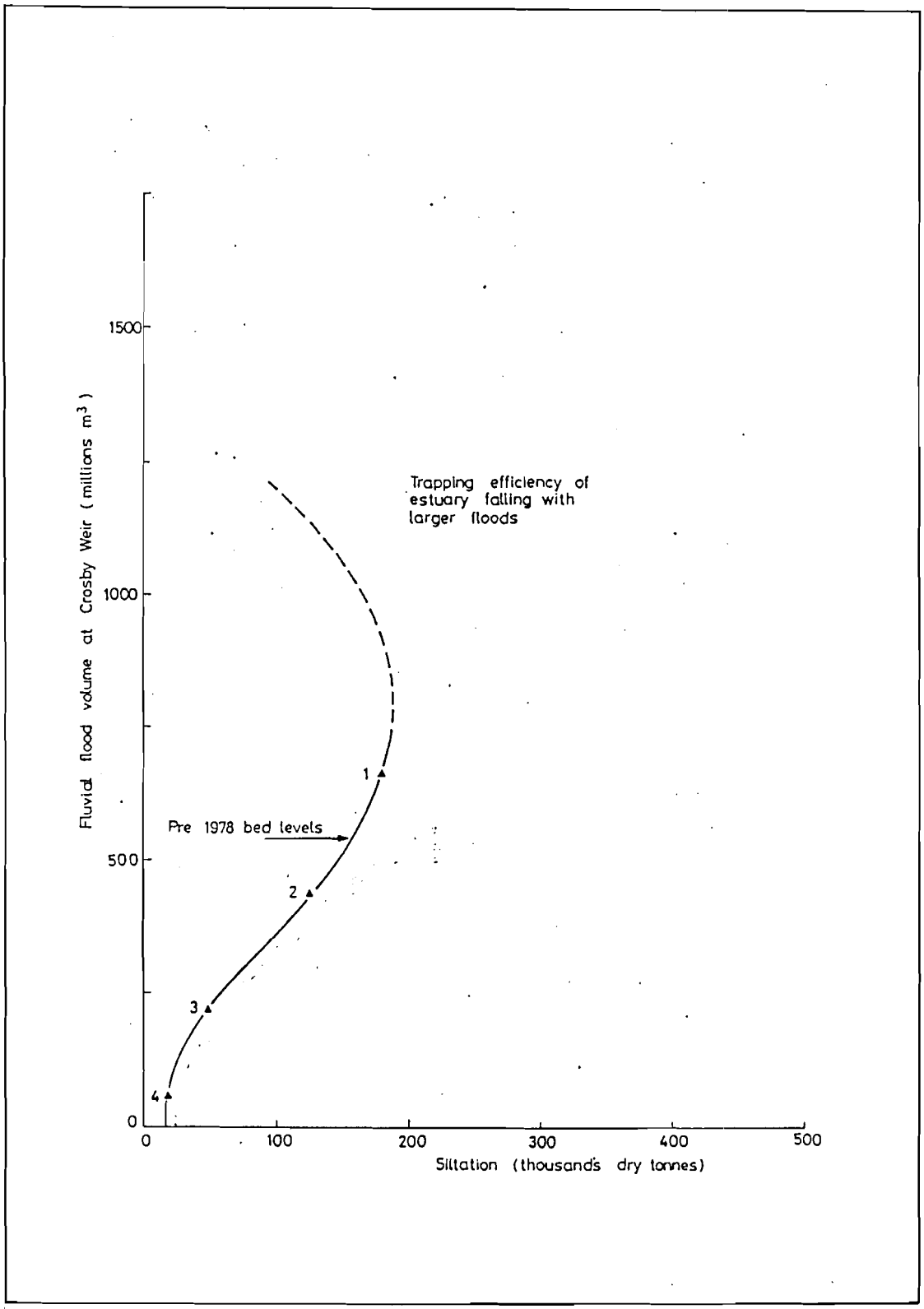

Fig 33 Net movement of mud into the estuary as a function of fluvial flood volume